SGP-TR-68

Geothermal Reservoir Evaluation Considering Fluid Adsorption and Composition

Michael J. Economides

September, 1983

Financial support was provided through the Stanford Geothermal Program Contract No. DE-AT03-80SF11459 and by the Department of Petroleum Engineering, Stanford University

Stanford Geothermal Program
Interdisciplinary Research in
Engineering and Earth Sciences
STANFORD UNIVERSITY
Stanford, California

GEOTHERMAL RESERVOIR EVALUATION CONSIDERING FLUID ADSORPTION AND COMPOSITION

A DISSERTATION

SUBMITTED TO THE DEPARTMENT OF PETROLEUM ENGIN'EERING

AND THE COMMITTEE ON GRADUATE STUDIES

OF STANFORD UNIVERSITY

IN PARTIAL FULFILLMENT OF THE REQUIREMENTS

FOR THE DEGREE OF

DOCTOR OF PHILOSOPHY

By

Michael J. Economides

September 1983

I certify that I have read this thesis and that in my opinion it is fully adequate, in scope and quality, as a dissertation for the degree of Doctor of Philosophy.

Frank G. Miller

(Principal Adviser)

I certify that I have read this thesis arid that in my opinion it is fully adequate, in scope and quality, as a dissertation for the degree of Doctor of Philosophy.

Henry J Ramey Jr

I certify that I have read this thesis and that in my opinion it is fully adequate, in scope and quality, as a dissertation for the degree of Doctor of Philosophy.

William E Brigham

I certify that I have read this thesis and that in my opinion it is fully adequate, in scope and quality, as a dissertation for the degree of Doctor of Philosophy.

Roland N. Horne

Approved for the University Committee on Graduate Studies:

Dean of Graduate Studies and Research

ACKNOWLEDGEMENTS

To Prof. Frank G. Miller for his meticulous efforts, I owe a great deal.

Professors H.J. Ramey, Jr., and W.E. Brigham have done much to train my thinking process, along with that of many others who comprise the main thrust of reservoir engineering work in this nation.

Dr. Roland Horne, a friend as well as a professor at Stanford has encouraged me to continue this work when other obligations imposed on my time.

Finally, my wife, Professor Christine Ehlig-Economides with both her personal as well as professional presence saw me through a most difficult and demanding part of my life.

To all I owe my gratitude

Funding for this project was provided by the United States Department of Energy under subcontract 1673600 (Lawrence Berkeley Laboratory) and contract DE-AT03-80SF11459.

ABSTRACT

Previous reservoir engineering studies of vapor-dominated geothermal reservoirs have generally been analogous to conventional-model studies for natural gas reservoirs. One inconsistency in the existing work has been a discrepancy between the estimated quantity of stean-ic-place and the geological constraints on the estimated reservoir Sulk volume.

In this work, the concept that considerable adsorbed water may exist in a vapor-dominated zone is examined in detail. Experimental and theoretical evidence of adsorption phenomena is described. Then, the implications of adsorption on material balance calculations and on well test anslysis are determined by incorporating adsorption effects into existing models.

The resulting new methods of analysis provide a more realistic estimate of the nature and extent of the vapor-dominated zone. In particular, the new methods result in a considerable reduction in the estimsted formation thickness and suggest that the fracture porosity has been underestimated using conventional models for a naturally fractured reservoir.

In addition, the presence of noncondensable gas in the geothernal fluid has a profound effect on the thermodynaaics associated with vapor-liquid equilibrium and adsorption. Noncondensable gases can cause tho dew point pressure of a noncondensable gas-water mixture to be elevated as much as 80 psi, or more above the vapor pressure far pure water at the reservoir

temperature depending on the composition of the mixture. Hence, the presence of gas in the geothermal steam extends the pressure range where vapor adeorption phenomena are in effect. Monitoring of gas production in the produced geothermal fluids provides additional data useful in evaluating adsorption effects in the formation.

The importance of the adsorption phenomenon in reserve estimation is of a considerable magnitude. This work shows that a reserve estimate based on geologic evidence and the thermodynamic properties of steam could be as much as an order of magnitude lower than the actual mass of water present.

TABLE OF CONTENTS

LIST OF TABLES

LIST OF FIGURES

SECTION ONE

INTRODUCTION

Vapor-dominated geothermal reservoirs occur when the fluid pressure in the producing zone is at or below the saturation pressure corresponding to the reservoir temperature. Only a few geothermal fields in the world satisfy this criterion. These include The Geysers Field in northern California and the Larderello-Travale region in central Italy. Although they are few in number, the vapor-dominated geothernal reservoirs offer the most readily used form of geothermal fluid, namely high enthalpy steam used to power turbines for the generation of electricity.

Studies of reservoir and production behavior of vapor-dominated geothermal system have focused on estimates of resource size, reservoir longevity and resource management. Whiting and Ramey (1969) presented an application of material and energy balances to geothermal steam production. An important major work, early in the history of geothermal engineering, was an evaluation of the vapor-dominated Geysers Field by Ramey (1968). Applying conventional techniques for natural gas reservoirs, he attempted to estimate the reserves of steam-in-place. By also examining the net rate of heat loss, he concluded that the system was a closed, depletable resource. Thus, the stage was set for further reservoir engineering research.

While the natural gas analogy to geothermal steam reservoirs became an acceptable method of interpretation, the phenomenon of

"vapor pressure lowering" added a new dimension. Cady (1969), Bilhartz (1971), Strobel (1973) and Chicoine (1975) attempted to determine the minimum pressure at which liquid water was present in the porous medium. The first two reached the conclusion that vepor pressure lowering was not significant in unconsolidated silica sands, while the last two observed vapor pressure lowering in consolidated satdstones. The significance of their work is that for a given temperature liquid water would exist in vapor-dominated geothermal reservoirs at pressures below the saturation pressure of pure water.

Hsieh (1980, 1983), in a psrticulsrly original work that formed the basis for this work, designed an apparatus that allowed experiments to measure the adsorption phenomenon for water vapor at the high temperatures found in geothemal reservoirs. He quantified the amount of adsorbed water in both unconsolidated and consolidated sandstones and found adsorption to be significant.

Hsieh's work has shown that the adsorption phenomenon exists at all pressures below the saturation pressure and, hence, liquid and vapor coexist even at very low pressures. Hence, the term "vapor pressure lowering" is a misnomer.

As a consequence of the previous studies, it would appear that the treatment of a vapor-dominated geothermal system as one filled only by gas would greatly underestimate the ability of the reservoir rock to hold fluid. The presence of large quantities of adsorbed water must be taken into account in geothernal reservoir evaluation.

The purpose of this work is to incorporate the effects of the adsorption phenomenon into the conceptual models appropriate for

material balance and well test analysis calculations for vapor-dominated geothermal reservoirs.

Since vapor-dominated systems are rare, studies to evaluate them have been focused taking into account their particular geometries and fluid compositions. This work extends previous investigatiocs and provides new interpretations which appear to be more consistent with known information about the reservoir physics than previous studies.

The postulate that adsorbed water may be distributed throughout vapor-dominated reservoirs provided the basis for the methods developed here for material balance and transient pressure well test analyses. These models offer an alternative to the concept of an underlying boiling zone as the source of the fluid being produced.

In a subsequent section of this report adsorption phenomena of water and steam are discussed. Then, thermodynamic theory pertaining to noncondensable gas-water mixtures is developed and reviewed.

A new material balance equation is developed considering adsorption and the presence of noncondensable gases. Then, the Warren and Root (1963) model for naturally fractured reservoirs is extended to incorporate adsorption effects and provlde a new method for interpreting geothermal well tests. Finally, a numerical model is developed to test the validity of the assumptions made in the derivation of the analytical model based on Warren and Root (1963) theory.

There is a limitation associated with this work. Hsieh's (1983) experiments were done using unconsolidated and consolidated sandstone cores. Hence, the evaluation of the effects of the adsorption

phenonenon for particular reservoirs would require experimental results derived from cores from those reservoirs. Experimental work must be done to determine the actual magnitude of the adsorption phenomenon in each individual case. This is not a major limitation considering that the adsorbed fluid, as it will be shown later, may be the major source of production in vapor-dominated systems.

There are two obvious extensions to Hsieh's (1980) and this work: (1) experimental determination of the adsorption phenomenon using actual reservoir cores from vapor-dominated geothermal reservoirs, and (2) the investigation of the magnitude of the adsorption phenomenon in hydrocarbon systems. Hsieh found that at room temperatures, methane adsorption accounted for 6 percent of the quantity of gas in the pore space, while in the case of ethane, the adsorbed gas amounted to 25 percent of the total. Experimental work is needed to demonstrate the magnitude of the adsorbed hydrocarbon gases at temperatures and pressures commonly found in gas reservoirs.

If the importance of adsorption found in the case of steam were proven also for hydrocarbon systems, adsorption would become an important parameter in the evaluation of a newly found reservoir.

The next section will review the existing literature dealing with the evaluation of vapor-dominated geothermal systems, the implications of the special formation characteristics, fluid distribution and fluid composition.

SECTION TWO

LITERATURE REVIEW

An accelerated interest in geothermal energy as an alternative energy source brought about detailed studies of the reservoir physics. Kany of the ensuing developments applied classical reservoir engineering models. The work of Whiting and Ramey (1969) provided the framework for the material balance analysis in this work. An application of this aethod incorporating adsorption phenomena will be presented in Section Five.

In order to investigate the effects of adsorption on the flow behavior in the reservoir, it was necessary to choose conceptual models which would represent typical formation characteristics.

An important element of vapor-dominated geothermal formations is that the rock has very low permeability. Hence, this led investigators to focus on the flow characteristics of fractured systems. The model by Warren and Root (1963) for naturally fractured petroleum reservoirs was seen as an obvious basis for geothermal reservoir evaluation. The Warren and Boot model assumes that the formation consists of primary and secondary porosity. Flow in the formation occurs primarily through fractures, but the bulk of the fluid is stored within the intergranular matrix that makes up the primary porosity.

Mavor and Cinco (1979) extended the Warren and Root (1963) analysis to include wellbore storage and damage and constant producing pressure.

Considerable study was also devoted to the transient pressure behavior of geothermal wells which penetrate a natural fracture. The well test methods developed were intended to aid in the evaluation of reservoir characteristics below the completion zone. This derived from the fact that high formation temperatures can pose considerable hazards and technical problems relating to drilling through the entire pay thickness. Ramey and Gringarten (19'75) applied vertical fracture analysis to geothermal steam well behavior and analyzed well data from The Geysers Field.

However, conventional material balance and well testing techniques, when applied to vapor-dominated geothermal systems, result in unrealistically large estimates of the reservoir porosity-thickness product. A plausible geothermal reservoir model is the pnralielepiped model. Cinco et al. (1979) using source and Green's functions in a fashion first introduced by Gringarten and Ramey (1973), described a vapor-dominated geothemal reservoir enclosed by four vertical impermeable boundaries, an impermeable caprock and underlying boiling water. A boiling water zone below the vapor-dominated cone provides storage for a large mass of geothermal fluid available to producing wells. ?he parallelepiped model also offers an explanation of an essentially constant flowing pressure in some geothermal well tests. The model was applied by Barelli et al. (1978) to the Travale reservoir and by Economides et al. (1982) to The Geysers, resulting in the calculation of the vapor zone thickness and the three components of the permeability tensor.

Transient changes in the gas composition of produced steam constitutes another area of interest in several recent studies. Noncondensable gases consisting largely of carbon dioxide and hydrogen sulfide are common. Zyvolosky and O'Sullivan (1980) modeled the transport of carbon dioxide in a two-phase geothermal system. They concluded that monitoring of the gas content, especially in the early production history, is required for correct interpretation of pressure transients in geothermal fields with large gas contents. Sutton (1976) developed pressure-temperature curves for a two-phase system of water and carbon dioxide. These curves were used as input for a numerical model by Zyvolosky and O'Sullivan (1980). Also using the pressure-temperature curves of Sutton, Atkinson et al. (1978) attempted to interpret with thermodynamics, the extremely high gas content (primarily CO_2) of the Bagnore field in Italy. Finally, Grant (1979) developed a practical scheme to estimate the water content in a two-phase reservoir using the composition of the production fluid. An extensive analysis and a critique of these results appears in Section Four.

Herkelrath et al. (1983) modelled pressure transient behavior in vapor-dominated geothermal systems. They found experimentally that "the time required for steam-pressure transients to propagate through a core"..."was 10 to 25 times longer than predicted by conventional superhsated-steam-flow theory". They hypothesized that the phenomenon was caused by adsorption of steam in the porous medium and measured the extent of the adsorption phenomenon. A sink term was included in the conservation of mass equation, which was solved

numerically. Their solution was in excellent agreement with their experimental results.

The following section will deal with the adsorption phenomenon, its ramifications in a vapor-dominated geothermal reservoir and its relative magnitude when compared with the steam present.

SECTION THREE

ADSORPTION IN VAPOR-DOMINATED GEOTHERMAL FORMATIONS

Evidence in the literature (Derjeguin, 1966) suggests that gases in a porous medium are adsorbed on the grain surfsces. Water vapor in the presence of certain reservoir racks forms an adsorbed liquid layer in an otherwise vapor-dominated system. This indicates that current engineering methods for the evaluation of vapor-dominated geothermal reservoirs should be revised to include sdsorption.

To explore this matter, a brief review is made in this section of adsorption phenomena. Experimental and field data then are examined to evince the existence of this phenomenon in geothermal reservoirs. Finally, the amount of the adsorbed water and its magnitude relative to geothermal steam are examined.

3.1 The Adsorption Phenomenon

Evidence of water adsorption on a solid-liquid interface was presented by Henniker (1949). He reported that the depth of the surface zone, due to water adsorption, can extend for A thickness of several thousand Angstrom units depending on the liquid-solid combination. In particular, for water and silica, the water molecules are oriented for a thickness of 45 $\overset{o}{A}$, but for water and glass, the thickness is 5300 $\overset{o}{A}$. For purposes of comparison, typical pore diameters in a sandstone range from less than 3,000 to as high as 40,009 $\overset{o}{A}$ (Henniker, 1949).

Henniker also reported that the adsorbed water appeared to have a molecular orientation approaching that of a crystal. Horne et al.

(1968) reported that even in a bulk stream, water molecules are structured in clusters which are relatively stable with respect to temperature. The presence of silica in typical formation rocks, coupled with considerable surface area, suggests conditions leading to water adsorption.

Adsorption phenomena are not limited to water. Although nonpoiar liquids, including most oils, are largely unaffected by adsorption (Derjaguin, 1966), there is considerable evidence that gases, including hydrocarbon gases, and water vapor are subject to adsorption effects in porous media.

Brunauer, Emmett and Teller (1938) developed a device which is widely called the BET cell. It is used to measure the amount of adsorption that occurs for a gas on a solid material. The molecular structure of the adsorbed gas was not known, but the authors described the structure in much the same way that other investigators described the surface orientation of adsorbed liquid molecules. Further evidence is the fact that porosity measurements, using Boyle's law techniques, vary depending on the gas used. Because helium is an inert gas , such measurenents are considered most accurate when helium is used.

The work that was an inspiration for the research reported here was done by Hsieh (1980). He designed an apparatus for experiments similar to those done with the BET cell, but at the high temperatures required for a study of water-vapor adsorption phenomenon. Hsieh's results were presented as a series of adsorption/desorption isotherms such as the one shown in Fig. 3-1. The adsorption, X, is expressed

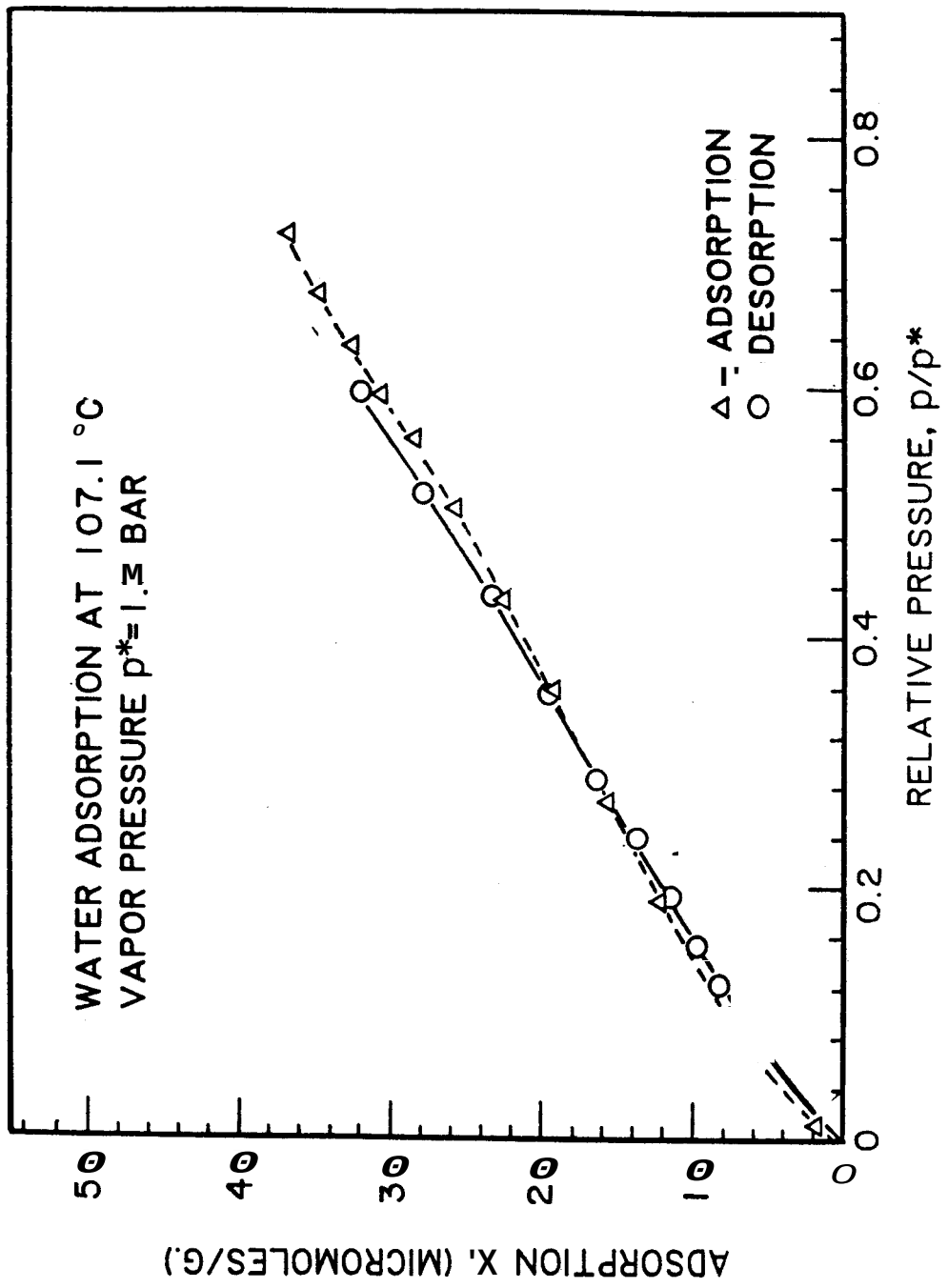

Figure 3-1 Adsorption-Desorption Isotherm for an Unconsolidated Core (From Hsieh, 1980)

in micromoles adsorbed per gram cf rock as a function of the relative pressure ratio p/p^*, where p^* is the vapor pressure. The data were approximately linear for experiments involving both unconsolidated sand and consolidated sandstones for temperatures ranging from 100 to 190°C. In all cases, the data formed lines converging at the origin disclosing that the mass of water adsorbed was nearly proportional to the relative pressure. Thus, the following equation can be applied as a close approximation:

$$X = \sigma p/p^* \qquad (3\text{-}1)$$

in which σ is a constant.

For unconsolidated sands, slope σ increases with temperature from 50×10^{-6} moles/g of rock at 100°C to 71×10^{-6} moles/g at 190°C. A graph of σ as a function of temperature is given in Fig. 3-2.

For consolidated sandstones, Hsieh found slope σ to be independent of temperature. For the Berea sandstone he studied, the value of σ was equal to 300×10^{-6} moles/g of rock.

He interpreted this difference in adsorption behavior as an indication that the predominant mechanism for adsorption in consolidate3 sandstone is micropore adsorption, while in sends, it is primarily due to surface adsorption.

Hsieh (1980) initially was attempting to demonstrate the phenomenon of "vapor pressure lowering". His work was preceded by

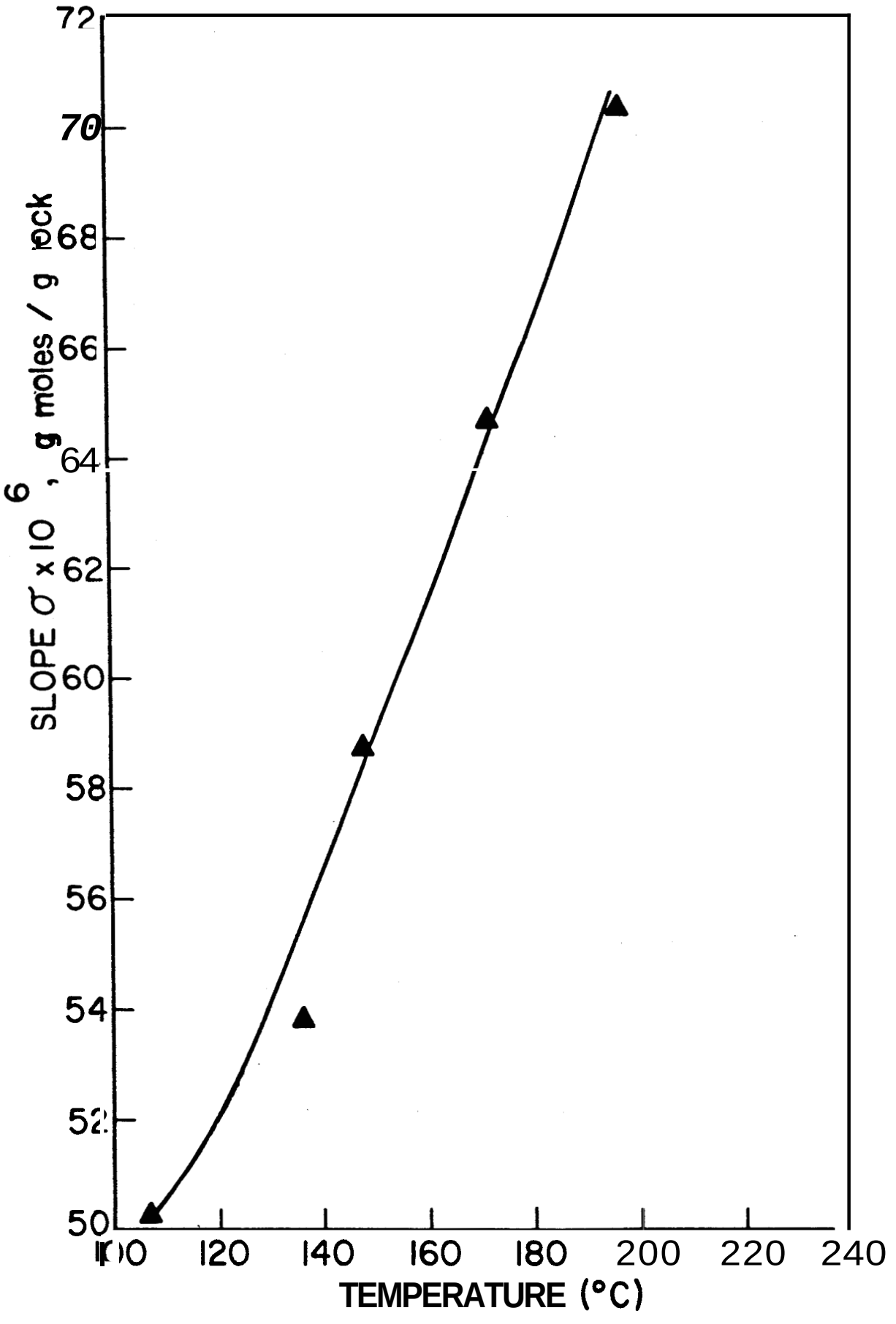

Figure 3-2 Adsorption Slope for Unconsolidated Cores (After Hsieh, 1980)

Cady (1969), Bilhartz (1971), Strobel (1373) and Chicoine (1975). Figure 3-3 shows sone results of Strobel (1973). Both Cady (1969) and Bilhartz (1971) concluded that the phenonenon was insignificant with unconsolidated sands, but that there was marked change in the vapor pressure in consolidated rocks.

In the present study, however, the term vapor pressure refers to the saturation pressure of pure water. This definition is necessary in order to model the effects of noncondenssble gases. Adsorbed water is distinguished from saturated liquid water. The term "vapor pressure" generally is defined as that pressure at which liquid and vapor of a pure substance coexist in equilibrium at a given temperature. The adsorption phenonenon, though, suggests that liquid and vapor coexist at all pressures below the saturation pressure for a given temperature.

Hence, the vapor pressure in a porous medium as used in this work is defined as the minimum pressure at which only liquid water exists. This pressure is the saturation pressure of the bulk fluid.

In a more recent study, Herkelrath and Moench (1983) measured the liquid water saturation in an unconsolidated, natural soil sample as a function of the vapor pressure. Again, approximately linear behavior was observed. The results of all these studies strongly suggest that adsorption of liquid water is present; in natural vepor-dominated geothermal reservoirs.

Although little work, if any, has been done on the adsorption effects of steam contaminated with noncondensable gases, Horne et al. (1968) observed that adsorbed water, at pressures exceeding the

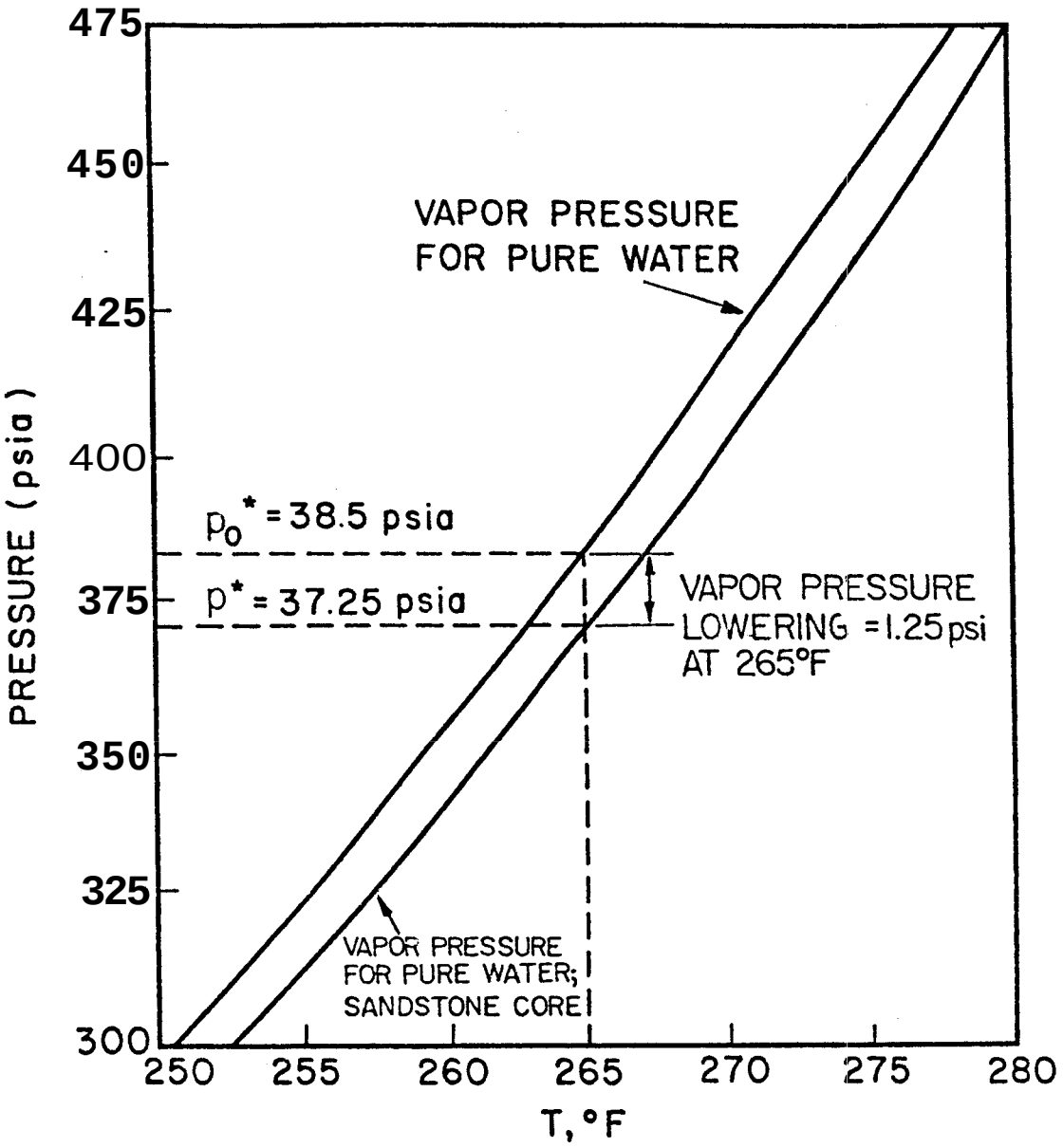

Figure 3-3 "Vapor Pressure Lowering" in a Sandstone Core.

(After Strobel, 1973)

saturation pressure, tended to exclude electrolytes from solution. Hence, normally soluble gases are assumed here to be largely insoluble in the adsorbed liquid phase. This point is discussed further in Sections Four and Five.

3.2 Field and Experimental Evidence Supporting the Existence of Liquid in a Vapor-Dominated Geothermal Reservoir

Evidence of liquid water present in a vapor-dominated reservoir has been supplied by other sources. Denlinger (1979), using detailed gravity, seismic and geodetic information for The Geysers, found that large masses of fluid were withdrawn over time from a zone approximately at the depth of The Geysers' vapor production zone. The reduction in mass far exceeded that which could be explained by production of the vapor. Yet, measured pressures in that zone are well below the saturation pressure at the reservoir temperature.

Another possible evidence of the adsorption phenomenon are the abnormally high neutron log porosities, measured in vapor-dominated geothermal formations, (Sanyal, 1980). Since the neutron log response measures hydrogen concentration a dense phase of adsorbed water may provide an explanation for the observed neutron log response.

Macias (1981) while measuring radon emanation in porous media, saturated with superheated steam, observed that the emanation level was considerably higher than the expected level from a porous medium saturated with a gaseous fluid. He postulated that the phenomenon was caused by the presence of a much denser adsorbed water phase.

3.3 The Magnitude of the Adsorption Phenomenon

The relationship between the quantities of adsorbed water and steam in a vapor-dominated reservoir can be calculated. The initial amount of adsorbed water can be obtained from Eq. 3-1 applied to the initial pressare p_i:

$$X_i = \sigma p_i / p^* \qquad (3\text{-}2)$$

For any particular bulk volume of porous rock, the volume of solid material present is m_r/ρ_r, $(1-\phi)V_b$ or $(1-\phi)V_p/\phi$. Thus, the pore volume available per unit mass of solid material can be expressed by:

$$\frac{V_p}{m_r} = \frac{\phi}{(1-\phi)\rho_r} \qquad (3\text{-}3)$$

Por a vapor-dominated system, adsorbed water would occupy a negligible portion of the pore volume. Hence, the mass of vapor present per unit of pore volume would be very nearly equal to the density of the vapor at the existing pressure and temperature. Symbolically $(m_g/V_p) = \rho_g = 1/v_g$ or:

$$m_g = \frac{V_p}{v_g} \qquad (3\text{-}4)$$

Solving Eq. 3-3 for $V_{P'}$ substituting the result for V_p in Eq. 3-4 and then rearranging yields the mass of vapor per unit mass of solid material. At the initial conditions of pressure (subscripted with an i) and temperature, assuming ρ_r constant:

$$\frac{m_{gi}}{m_r} = \frac{\phi}{(1-\phi)\rho_r v_{gi}} \qquad (3\text{-}5)$$

From Eq. 3-2 the mass of liquid adsorbed initially, expressed in gm per gm of solid material, is given by:

$$\frac{m_{ai}}{m_r} = \sigma \frac{p_i}{p^*} M_a \qquad (3\text{-}6)$$

Dividing Eq. 3-5 by Eq. 3-6 gives the vapor to adsorbed water mass ratio:

$$\frac{m_{gi}}{m_{ai}} = \frac{\phi m_r}{(1-\phi)\rho_r v_{gi} \sigma \frac{p_i}{p^*} M_a m_r} \qquad (3\text{-}7)$$

From Eq. 3-7, note that:

$$\frac{m_{ai}}{m_{gi}} = \frac{M_a \rho_r (1-\phi) v_{gi} (\sigma p_i/p^*)}{\phi} \qquad (3\text{-}8)$$

Equation 3-8 is general. For a geothermal reservoir near its saturation point and at a typical temperature of 450°F, the ratio p_i/p^* approaches unity, while v_g is approximately equal to one ft^3/lb in English engineering units. Assuming for common geothermal rocks that the density can be approximated as 2.65 g/cc or 165 lb/ft^3 and the value of σ as 300×10^{-6} lb moles/lb of rock, Eq. 3-8 becomes:

$$\frac{m_{ai}}{m_{gi}} \approx 0.893 \frac{1-\phi}{\phi} \qquad (3\text{-}9)$$

This equation has an important implication. In a vapor-dominated system for very low values of the porosity, there can be considerable mass-in-place in the form of adsorbed water. For example, for a porosity of 5%, the ratio, m_{ai}/m_{gi}, is approximately equal to 17, that is, there may be as much as 17 times more adsorbed water in the formation than vapor (by mass).

The next section will deal with the thermodynamics of the H_2O-CO_2 system and will present information that will be used in subsequent sections dealing with the evaluation of geothermal reservoirs containing CO_2.

SECTION FOUR

THERMODYNAMICS OF THE WATER-CARBON DIOXIDE SYSTEM

The presence of carbon dioxide in geothermal systems is common. The Broadlands field in New Zealand produces about 10% (mole) CO_2, Travale in Italy about 11% CO_2, while the Bagnore field posted an initial noncondensable gas composition of over 80%. In this section, the thermodynamics of the water-carbon dioxide systems is studied. While geothermal reservoirs generally contain many other gases including H_2S, NH_3 and CH_4, the concentration of CO_2 in the noncondensable gas mixture is usually over 90%. Although there are substantial data on the H_2O-CO_2 system, data on H_2O-noncondensable gas sixtures are scarce. Since CO_2 is by far the major component, the study of H_2O-CO_2 systems may be considered a reasonable first represestation of the total system.

The first item to be considered is the distribution of CO_2 in a vapor-dominated geothermal reservoir. The presence of CO_2 causes an elevation of the mixture dew point pressure. A mixture that contains water and a much higher vapor-pressure fluid (such as CO_2) has a dew point pressure curve significantly higher than the boiling curve for pure water. Hense, a major effect of the presence of carbon dioxide in a geothemal fluid is to allow a vapor phase to exist at pressures significantly higher than the saturation pressure of pure water.

Since adsorption effects, discussed in the previous section, apply below the vapor pressure of pure water, the presence of the CO_2

(noncondensable gases) extends the pressure range where adsorption effects prevail above the pure water vapor pressure.

Finally, the assumption that appears throughout this report that the depletion of a vapor-dominated geothermal: reservoir may be considered as isothermal is examined.

4.1 Carbon Dioxide Distribution in a Vapor-dominated Geothermal Reservoir

Because noncondensable gases (primarily CO_2) are soluble in water, the reservoir noncondensable gas content partitions itself between the liquid and vapor phases, (Grant, 1979).

Sutton (1976), while presenting boiling curves for a two-phase mixture of wster and carbon dioxide, calculated the amount of CO_2 dissolved in water. In the region of geothermal interest, the CO_2 mole fraction in the liquid phase is in the range of 5×10^{-4} to 10^{-3} (or 1.22×10^{-3} to 2.44×10^{-3} mass fraction).

Grant (1979) used the presence of carbon dioxide and hydrogen sulfide to calculate the water content in the Kawah-Kamojang geothermal reservoir in Indonesia (a two-phase reservoir with a steam cap). In that reservoir, the CO_2 content in the produced fluid initially was approximately 1% (mass). This was assumed to be equal to the initial concentration in the vapor phase. Grant calculated that the water saturation in the Kawah-Kamojang reservoir was 35%. Using Sutton's (1976) and Grant's (1979) data, the distribution of CO_2 in the Kamojang reservoir can be calculated. Since the reservoir temperature was 240°C (464°F), the specific volumes of vapor and liquid were $v_g = 0.957$ ft^3/lb, and $v_\ell = 0.0197$ ft^3/lb

respectively. Using a unit pore volume as a basis, the weight of vapor present would be (0.65/0.957) lb or 0.68 lb and the weight of liquid water present would be (0.35/.0197) lb or 17.76 lb. From the production data, as reported by Grant (1979), the amount of CO_2 present in the vapor phase was then 0.68 x 0.01 = 6.8 x 10^{-3} lbs/ft^3 of pore volume, while the amount in the liquid phase was at least 17.76 x 1.22 x 10^{-3} = 21.67 x 10^{-3} lbs. Hence, in the Kawah-Kamojang two-phase geothermal reservoir, the CO_2 mass in the liquid phase was approximately three times the CO_2 mass in the vapor phase.

In a vapor-dominated geothermal reservoir, the only "non-vapor" fluid present is in the form of adsorbed water. In the last section, we observed that adsorbed water does not exhibit the same properties as free water. In particular, the ordered molecular structure of the adsorbed water reduces the concentration of any water soluble gases significantly.

In the example presented at the end of Section Three, for a porosity equal to 0.05, the mass ratio of the adsorbed water to the steam was approximately equal to 17. According to Sutton's (1976) calculation, the mass fraction of CO_2 dissolved in liquid water in the region of geothermal interest is in the range of 1.22 x 10^{-3} to 2.44 x 10^{-3}. Using the results of the example presented in Section Three, for a basis of 18 lbs of total fluid (including adsorbed water and steam), there could be 17 x 1.22 x 10^{-3} ≤ 0.02 lbs of CO_2 in solution.

The equilibrium constant calculated from Sutton's (1976) correlation for 450°F and for a pressure near the saturation point of water is approximately equal to 280.

Hence, the mass fraction of CO_2 in the vapor phase is equal to 0.34. For the calculation at hand (and using a basis of 18 lbs of total fluid of which 1 lb is vapor), the C02 concentration in the vapor phase is 0.34 lbs. Hence, the mass ratio of CO_2 dissolved in the adsorbed water to the CO_2 in the vapor phase is equal to 0.06 compared to a ratio of 3 calculated for the two-:phase Kawah-Kamojang system and using Grant's (1979) data.

From the above, it can be concluded that proportionately there is far less C02 dissolved when adsorbed water is the only "non-vapor" fluid present. There is a further consideration. The compactness of the molecular layers of the adsorbed water would preclude the psssibility that basic principles of vapor-1iqui.d equilibrium would apply between the adsorbed water and the overlying steam and CO_2 mixtures. The equilibrium constant, K, would be much larger in adsorbed water/CO_2 equilibrium than in bulk water/CO_2 equilibrium, since the solubility of CO_2 in the adsorbed water should be far less than that in non-adsorbed water.

Also in the last section, the mass of adsorbed water per mass of rock was estimated from the results of Hsieh (1980). For a given matrix porosity, the mass of the adsorbed water can be estimated.

Equation 3-8 relates the mass ratio, m_{ai}/m_{gi}, of adsorbed water to the vapor.

$$\frac{m_{ai}}{m_{gi}} = \frac{M_a \rho_r (1-\phi) v_g (\sigma p_i / p^*)}{\phi} \qquad (3\text{-}8)$$

This ratio, depending heavily on the reservoir porosity, ranges from 1 to 20 for conditions expected in geothermal reservoirs. In any case, the ratio is much smaller than the ratio of liquid water to steam found in two-phase systems. The small mass fraction of adsorbed water in a vapor-dominated system, coupled with a postulated limited ability of CO_2 to dissolve in adsorbed water, is the basis for considering that in a vapor-dominated geothernal reservoir, all of the CO_2 (and effectively all other noncondensable gases) are in the vapor phase. This should be a reasonable first approximation.

4.2 Dew Point Pressure Elevation in Vapor-dominated Water-Carbon Dioxide Systems

In calculating the dew point pressure of a vapor-dominated geothernal system, the assumptions are:

1. All CO_2 is in the vapor phase.
2. Any liquid present is in the form of adsorbed water.

The equilibrium condition for a dew point pressare at a given temperature is:

$$\sum z_i / K_i = 1 \qquad (4\text{-}1)$$

or in the case of a CO_2/water mixture:

$$\frac{z_{CO_2}}{K_{CO_2}} \quad \frac{z_{H_2O}}{K_{H_2O}} = 1 \qquad (4\text{-}2)$$

Malinin (1974) reports that in the region of geothermal interest, the fugacity coefficients of the H_2O-CO_2 system approach unity. Therefore, Dalton's and Raoult's law can be assumed as applicable for the system. The equilibrium constant of water vapor can, therefore, be approximated by:

$$K_{H_2O} = p^*_{H_2O}/p_{total} \qquad (4\text{-}3)$$

The equilibrium constant for CO_2 can be obtained from Sutton's (1976) fit of four sets of experimental data. Figure 4-1 presents the experimental data of Ellis and Golding (1936), Malinin (1959), Todheide and Franck (1963) and Takenouchi and Kennedy (1964). Sutton's fit of the experimental data is represented by the solid line. The fitted equation is:

$$(K_{CO_2} p)^{-1} = [13.27 - 8.54(T/100) + 2.93(T/100)^2] \times 10^{-5}$$

(4-4)

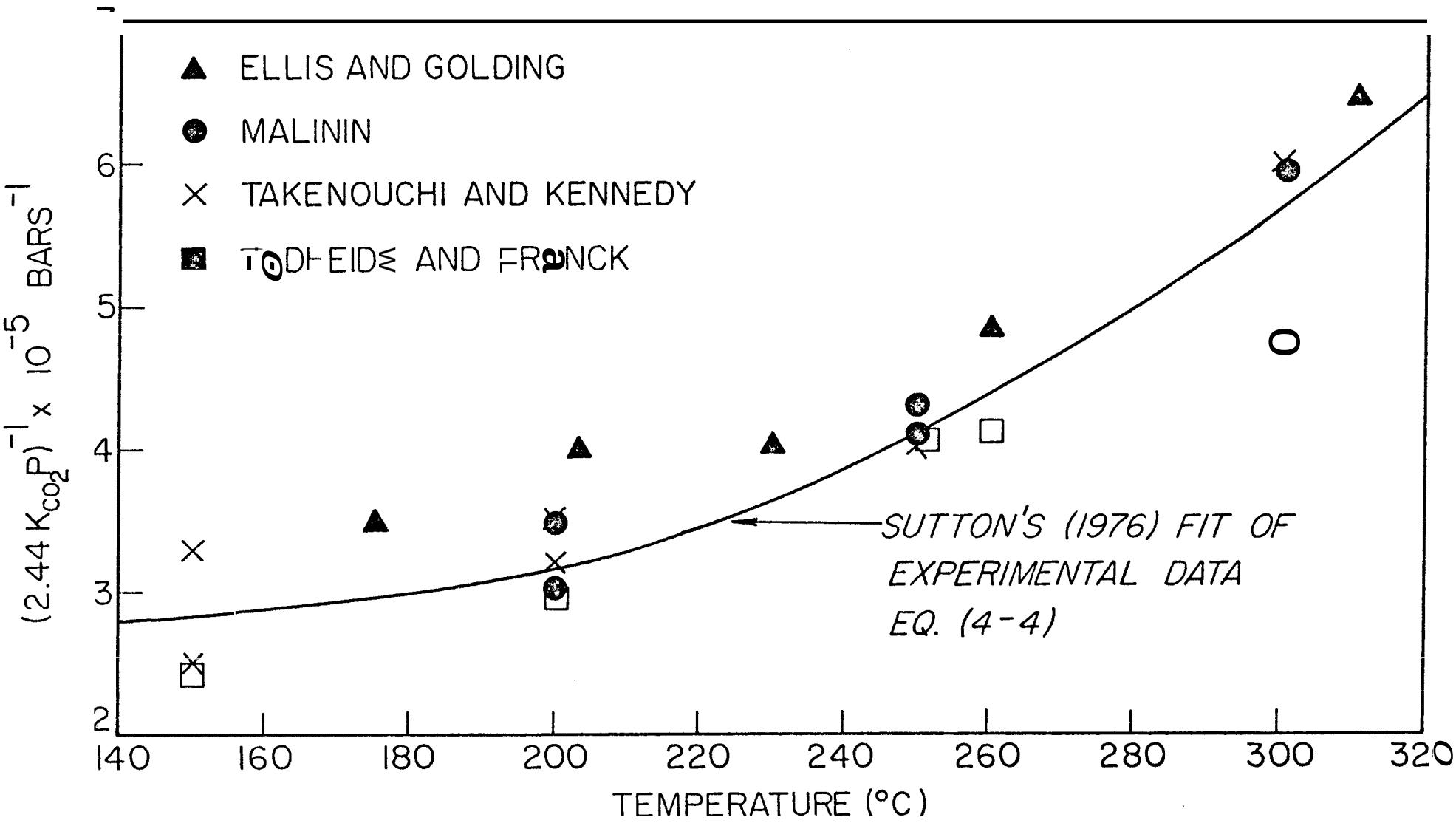

Figure 4-1 The Vapor-Liquid Equilibrium Constant for H_2O-CO_2 System.

where p is total pressure in bars and T is in ^{o}C.

The constants in Eq. 4-4 vary from the one presented by Sutton by a multiplier equal to 2.44 which is to account for the definition of the equilibrium constant as a mole fraction ratio. Sutton's curve was for mass ratios.

In English engineering units, Sutton's equation can be transformed into:

$$(K_{CO_2}\, p)^{-1} = [10.02 - 3.20(T/100) + 0.61(T/100)^2] \times 10^{-6} \qquad (4\text{-}4a)$$

where pressure and temperature are in psi and ^{o}F, respectively.

Equations 4-2 and 4-3 can be combined:

$$\frac{z_{CO_2}}{K_{CO_2}} \quad \frac{z_{H_2O}\, p_{total}}{+\ p^*_{H_2O}} = 1 \qquad (4\text{-}5)$$

The numerator and denominator of the first term on the left side of the equation are multiplied by p_{total}. Rearrangement results in:

$$p_{total} = 1 \Big/ \left[\frac{z_{CO_2}}{K_{CO_2}\, p_{total}} + \frac{z_{H_2O}}{p^*_{H_2O}} \right] \qquad (4\text{-}6)$$

Tnis equation provides the total pressure for an H_2O-CO_2 mixture if the product concentrations an3 the reservoir temperature are known. Tne value of the prsduct ($K_{CO_2}\ p_{total}$) may be obtained from Eq. 4-4 or 4-4s, which is Sutton's (1976) correlation of several sets of experimental dsta.

The saturation pressure of pure water can be obtained from steam tables. A convenient correlation developed for this study for the saturation pressure of pure water in the range of geothermal interest is:

$$p^* \doteq 3.76 \times 10^{-10}\ T^{4.54} \qquad (4\text{-}7)$$

in which p^* is in psia and T in ^oF. Equation 4-7 was derived from a least squares polynomial: fit of the steam vapor-pressure curve in the range between 200°F and 600°F.

Using Eqs. 4-4a, 4-6 and 4-7, the dew point pressure of H_2O-CO_2 mixtures can be calculated.

Example 4.1 Vapor-pressure elevation of a CO_2-H_2O mixture

Assume a vapor-dominated geothermal reservoir at 450°F (232°C) containing 15% (weight) of CO_2. Calculate the total pressure of the system.

The mole fraction of CO_2 is:

$$z_{CO_2} \doteq \frac{0.15/44}{(0.15/44) + (0.85/18)} \doteq 0.067 \qquad (4\text{-}8)$$

Using Eq. 4-7 the vepor pressure, $p^* \simeq 418$ psia compared to 422 psia in the Steam Tables. From Eq. 4-4a, the product $K_{CO_2}p$ is calculated:

$$K_{CO_2}p \simeq 1.25 \times 10^5 \text{ psi} \qquad (4\text{-}9)$$

Finally, using Eq. 4-6, $p_{total} \simeq 448$ psia, which represents an elevation of 30 psia over the vapor pressure.

Figure 4-2 presents the calculated vapor-pressure elevation of CO_2-H_2O mixtures for various C02 concentrations. The elevation is significant. For regions of geothermal interest,, the total pressure of the system may be 60-90 psi higher than the saturation pressure of pure water for fairly moderate CO_2 concentrations. High CO_2 concentrations, as in the Bagnore region of Italy, may elevate the pressure further and still sustain the mixture in the vapor phase.

A conjecture may be made here. The adsorption phenomenon is assumed to continue the same trend as with pure steam. The surface forces causing the adsorption phenomenon are assumed not to be affected by the CO_2 presence. So, while little CO_2 is believed to be dissolved in the adsorbed liquid, its presence, by elevating the dew point pressure above p^*, extends the adsorption phenomenon further. The curve of Fig. 3-1 for adsorbed water versus p/p^* is extrapolated with the same slope σ for $(p/p^*)>1$.

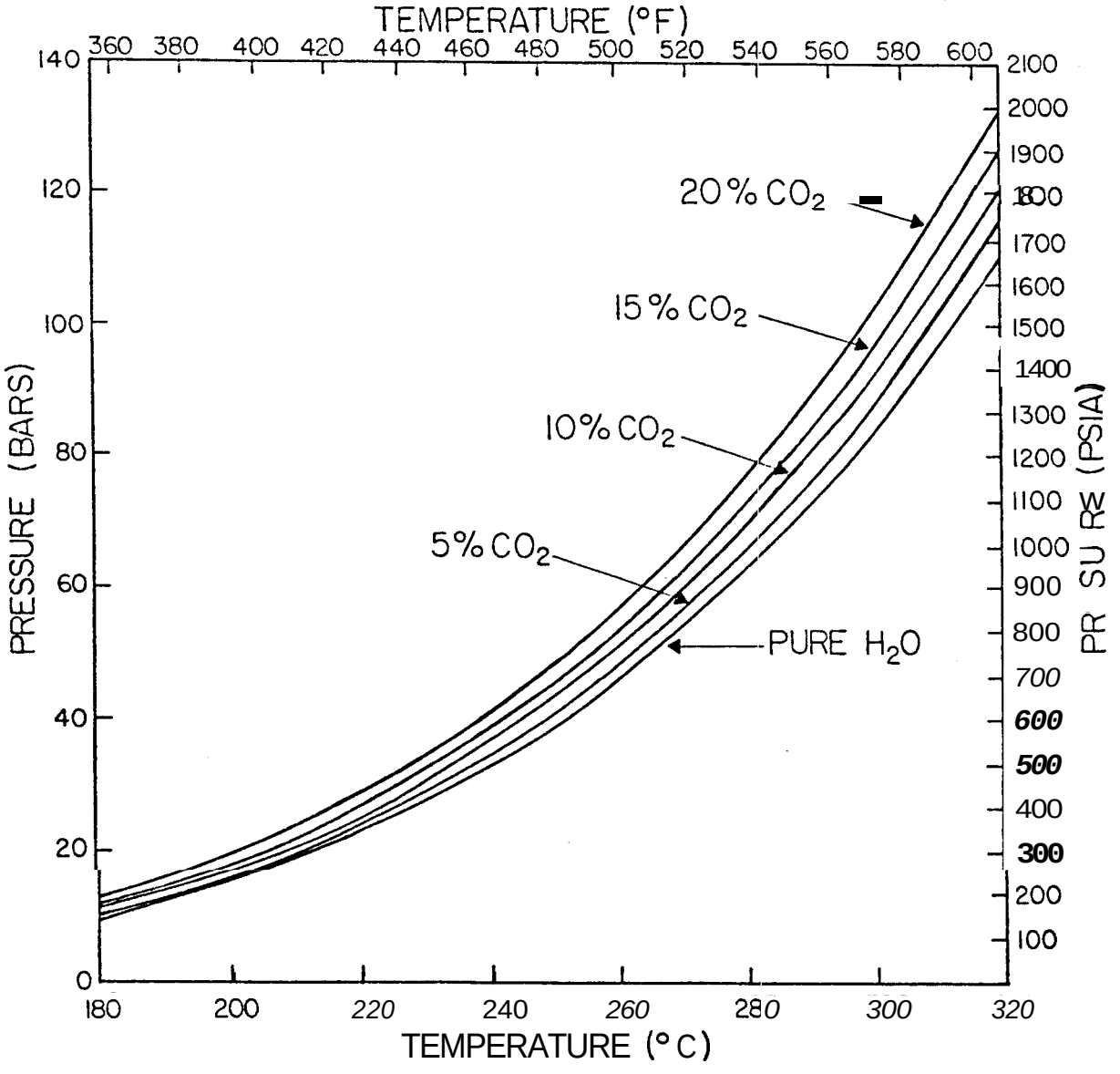

Figure 4-2 Dew Point Pressure Elevation in the H_2O-CO_2 System,

Further, the assumption that the CO_2 concentration in the adsorbed liquid phase is negligible implies that as water is desorbed during production, the concentration of CO_2 in the vapor and hence in the production stream, should be diluted if adsorbed water were the only "non-vapor" fluid present. Existence of liquid beneath the vapor-dominated zone may, in fact, cause the [increase of the CO_2 concentration produced as it boils out of the mixture. The implications of the dilution of the CO_2 concentrstion are treated in Section Five.

4.3 The Temperature Decline of a Vapor-:Dominated Geothermal Reservoir Considering Adsorption

Whiting and Hamey (1969) presented a material end energy balance for a vapor-dominated reservoir. Brigham and Morrow (1974) offered a calculation procedure to predict the pressure and temperature versus production history for such reservoirs. In Ramey's (1968) work for The Geysers, he presented a simplified energy balance for a depleting vapor-dominated reservoir. The expression for the energy balance was:

$$(W_p + W_L)(h_p - F) + W_i \left(h_i + v_i \frac{(1-\phi)}{\phi} \rho C (T_i - T) - F - \frac{v_i h_{\ell g}}{v_g - v_\ell} \right) + W_e (h_e - F) + Q_s \qquad (4\text{-}10)$$

where

$$F = h_{\ell} - \frac{h_{\ell g} v_{\ell}}{v_g - v_{\ell}} \qquad (4\text{-}11)$$

and

$$v_i = x_i (v_{gi} - v_{\ell i}) + v_{\ell i} \qquad (4\text{-}12)$$

Assuming a closed system, the fluid lost, W_L and the fluid influx, W_e may be set equal to zero. Further, Ramey (1968) has shown that the net heat conducted into the reservoir, Q_s is negligible. Therefore, Eq. 4-10 may be simplified and rearranged into:

$$T_i - T = \frac{\frac{W_p}{W_i}(h_p - F) - h_i + F + \frac{v_i h_{\ell g}}{v_g - v_{\ell}}}{v_i \frac{(1-\phi)}{\phi} \rho_r C_r} \qquad (4\text{-}13)$$

Equation 4-13, providing the temperature drop must be solved by trial and error since the thermodynamic variables in the right-hand side are functions of the current reservoir temperature, T. In Section Three, Eq. 3-9 provided the initial mass ratio of adsorbed water to the vapor for a typical vapor-dominated geothermal reservoir. In the example at the end of the section, using a porosity of 0.05, the mass ratio was found to be approximately equal

to 17 yielding an initial fluid quality of 1/18 if vapor and adsorbed water were lumped together.

Equation 4-12 then becomes:

$$v_i = \frac{1}{18}(1.0993-0.0194) + 0.0194 = 0.0734 \text{ ft}^3/\text{lb} \qquad (4\text{-}14)$$

(The values for the vapor and liquid specific volumes and all other initial variables are for saturated fluid at 450°F as in the example in Section Three).

Using $\rho_r = 165 \text{ lb/ft}^3$ and $C_r = 0.25 \text{ BTU/lb}^\circ\text{F}$, Eq. 4-13 may then be solved by trial and error.

For a depletion $W_p/W_i = 0.25$, and for a produced fluid enthalpy equal to the average steam enthalpy in the reservoir during the operation, the calculation yields a temperature decline of 3°F. A porosity of 0.20 yields a temperature decline of 6°F. Hence, the contention throughout this report that the depletion of a vapor-dominated geothermal reservoir may be considered as isothermal is a good approximation.

SECTION FIVE

MATERIAL BALANCE FOR VAPOR-DOMINATED GEOTHERMAL RESERVOIRS

?he presence of carbon dioxide and adsorbed water has a major effect on material balance calculations for vapor-dominated geothermal reservoirs.

In this work, four material balance models are investigated:

1. Conventional material balance for steam reservoirs analogous to balances for natural-gas reservoirs.
2. Steam and noncondensable gas reservoirs.
3. Steam and adsorbed water reservoirs.
4. Steam, adsorbed water, and noncondensabke gas reservoirs.

In this section, examples will be presented which show how the various models apply to The Geysers and to various Italian geothermal reservoirs.

5.1 Conventional Material Balance for the Steam Reservoir

Ramey (1968) applied the conventional material bslance model for a natural gas reservoir to the vapor-dominated geothermal: reservoir at The Geysers. In a graph of p/Z versus cumulative production, he showed that the data for the first 10 years indicated a straight-line relationship for $W_p > 20 \times 10^9$ lbs (Fig. 5-1). He presented a volumetric balance for a steam reservoir when only superheated steam is considered. This balance can be expressed as:

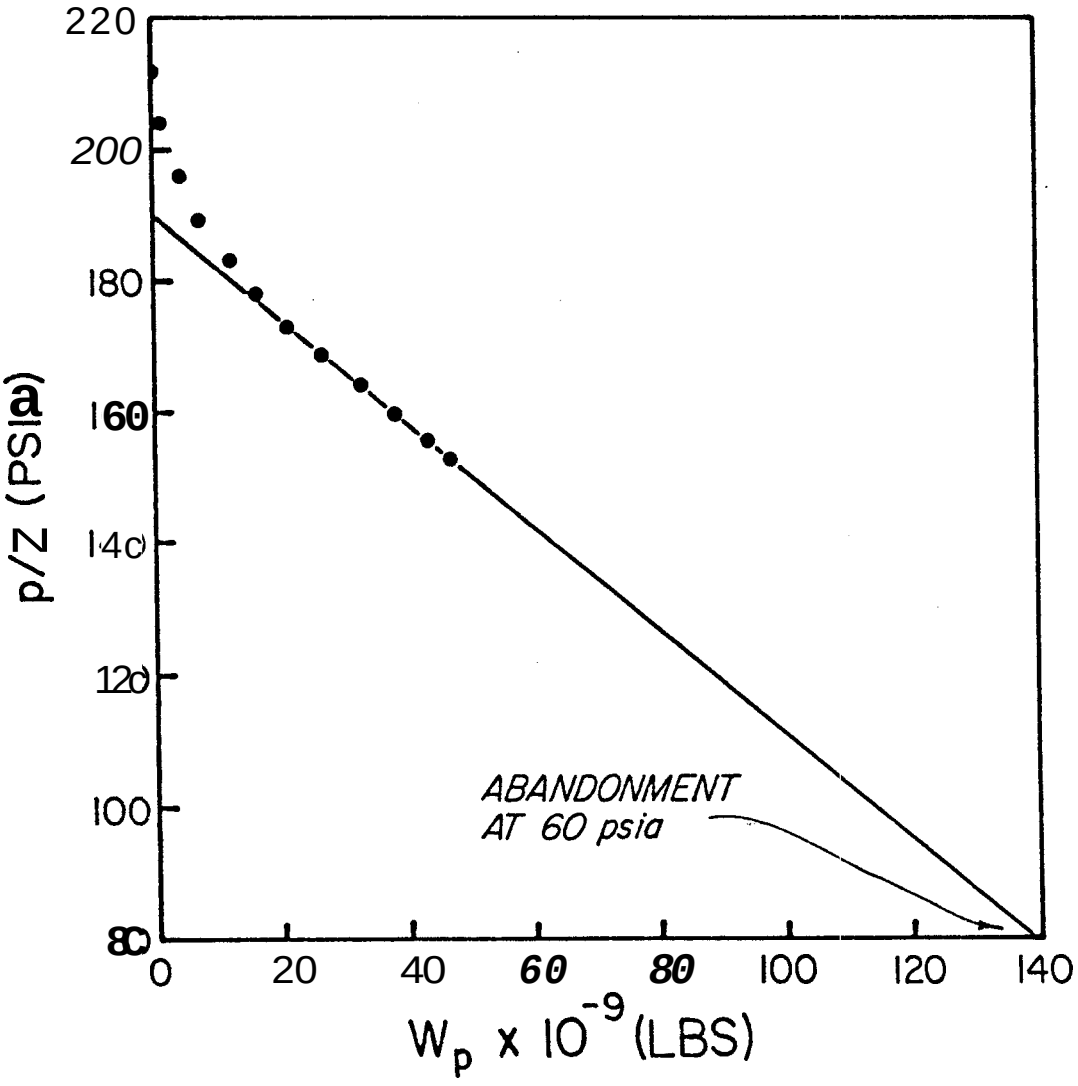

Figure 5-1 p/Z vs. Cumulative Production for the Big Geysers Zone.

(After Ramey, 1968 Modified)

$$\text{(Reservoir pore volume)} = W_i v_{gi} = (W_i - W_p) v_g \qquad (5\text{-}1)$$

from which:

$$W_p v_g = W_i (v_g - v_{gi}) \qquad (5\text{-}2)$$

where W_p is the mass cumulative production, W_i is initial mass-in-place, and v_g is the vapor specific volume at reservoir conditions. The latter may be derived from the real gas law:

$$v_g = \frac{ZRT}{Mp} \qquad (5\text{-}3)$$

Vapor-dominated geothermal reservoirs have been treated as isothermal through most of the conventional reservoir engiceering literature. They are treated as such here as well. Equation 5-2 then becomes:

$$W_p = W_i - \frac{Z_i W_i}{p_i} (p/Z) \qquad (5\text{-}4)$$

which is the equation Ramey used in getting the straight line relationship shown in Fig. 5-1.

Referring to Eq. 3-3, the pore volume per unit mass of solid rock material is given by:

$$\frac{V_r}{m_r} = \frac{1}{(1-\phi)\rho_r} \qquad (3\text{-}3)$$

The mass of vapor contained in pore volume, V_p is then:

$$W = \frac{\phi m_r}{(1-\phi)\rho_r v_g} \qquad (5\text{-}5)$$

Combining Eqs. 5-4 and 5-5:

$$\frac{W_p}{m_r} = \frac{M\phi}{(1-\phi)\rho_r RT}\left(\frac{p_i}{Z_i} - \frac{p}{Z}\right) \qquad (5\text{-}6)$$

The value of the molecular weight, M, is equal to 18 since only water vapor is considered here.

As with the conventional natural gas technique (Eq. 5-4), the procedure suggested by Eq. 5-6 is a graph of cumulative production versus p/Z. Theoretically, a straight line drawn through the data would provide the initial-steam-in-place at the ,intercept with p/Z = 0.

The application of a conventional material balance to The Geysers field by Ramey (1968) resulted in a very large value for the initial steam-in-place. It will be demonstrated later in this section that if one were to assume a steam zone with no adsorbed water present it would lead to the calculation of an unrealistically high value for the formation thickness whether or not the steam zone is underlain by subformation liquid.

The presence of adsorbed water, as will be shown, provides a means for storage of the estimated mass within a more reasonable thickness.

5.2 Steam and Noncondensable Gas Reservoirs

The presence of noncondensable gases, as pointed out earlier, results in the elevation of the dew-point pressure. A material balance equation, similar to Eq. 5-1, can be written for all steam and noncondensable gases found in the reservoir:

$$W_p \sum_{1}^{k} m_k v_{gk} = W_i \sum_{1}^{k} m_k (v_{gk} - v_{gik}) \qquad (5\text{-}7)$$

In Eq. 5-7, the cumulative production and the initial mass-in-place are in terms of total mass, while the various components ere included by their mass fraction, m_k. Equation 5-7 assumes that Amagat's law of additive volumes is applicable for the conditions commonly found in vapor-dominated geothermal reservoirs.

Although Eq. 5-7 is general in nature, it can be simplified by lumping the noncondensable gases:

$$W_p(m_{NC}v_{NC} + (1 - m_{NC})v_{H_2O}) =$$

$$W_i(m_{NC}(v_{NC} - v_{NCi}) + (1 - m_{NC})(v_{H_2O} - v_{iH_2O})) \qquad (5\text{-}8)$$

Substitution of the equivalent expressions for the specific volumes, as given by Eq. 5-3 and rearrangement, results in:

$$W_P = W_i \left| 1 - \frac{\frac{m_{NC} Z_{NCi}}{M_{NC} p_i} - \frac{(1 - m_{NC}) Z_i}{M_{H_2O} p_i}}{\frac{m_{NC} Z_{NC}}{M_{NC} p} + \frac{(1 - m_{NC}) Z}{M_{H_2O} p}} \right| \qquad (5\text{-}9)$$

For simplicity and consistency with other equations, the subscript "H_2O" in Eqs. 5-8 and 5-9 will be omitted in equations which follow. The noncondensable gas fraction m_{NC} is a cumulative term including all gases. In most cases, this term very nearly equals the mass fraction of CO_2, because of the high CO_2 content (90% mole or more) in most geothermal reservoirs.

The initial-mass-in-place per unit mass of rock may be obtained by analogy with Eq. 5-5:

$$W_i = \frac{\phi m_r}{(1-\phi)\rho_r [m_{NCi} v_{NCi} + (1 - m_{NCi}) v_{gi}]} \qquad (5\text{-}10)$$

Substitution of Eq. 5-3 in Eq. 5-10, combined with Eq. 5-9 and rearrangement results in:

$$\frac{W_p}{m_r} = \frac{\phi}{(1-\phi)\rho_r RT} \left\{ \frac{p_i/Z_i}{\frac{m_{NC} Z_{NCi}}{M_{NC} Z_i} + \frac{(1-m_{NC})}{M}} - \frac{p/Z}{\frac{m_{NC} Z_{NC}}{M_{NC}} + \frac{(1-m_{NC})}{M}} \right\} \qquad (5\text{-}11)$$

Equation 5-11 reduces to 5-6 if $m_{NC} = 0$. The value of Z_{NC} may be considered unity for gases at pressures in the range of geothermal interest. This contention may be verified through the following calculation: From Fig. 15-11 on page 577 of Katz et al (1959) Handbook of Natural Gas Engineering, the critical pressure (p_c) of CO_2 is estimated to be 1075 psia and the critical temperature (T_c) is 88°F, or 548°R. Assuning a reservoir temperature of 464°F or 924°R and a reservoir pressure of 500 psia, the corresponding reduced temperature and pressure are:

$$T_r = \frac{T}{T_c} = \frac{924}{548} = 1.69$$

and

$$p_r = \frac{p}{p_c} = \frac{500}{1075} = 0.465$$

From the Z chart (Fig. 4-16 in Katz et al) $Z \simeq 0.975$. Equation 5-11 is no longer a straight line since the p/Z parameter is divided by a pressure dependent quantity.

Figure 5-2 shows a material balance calculation for geothermal reservoirs containing various concentrations of noncondensable gases. The calculation was done for a temperature of 450°F. As can be seen, the p/Z versus cumulative production curves are slightly curving, the curvature becoming more pronounced as the noncondensable gas content increases. For geothermal reservoirs where the

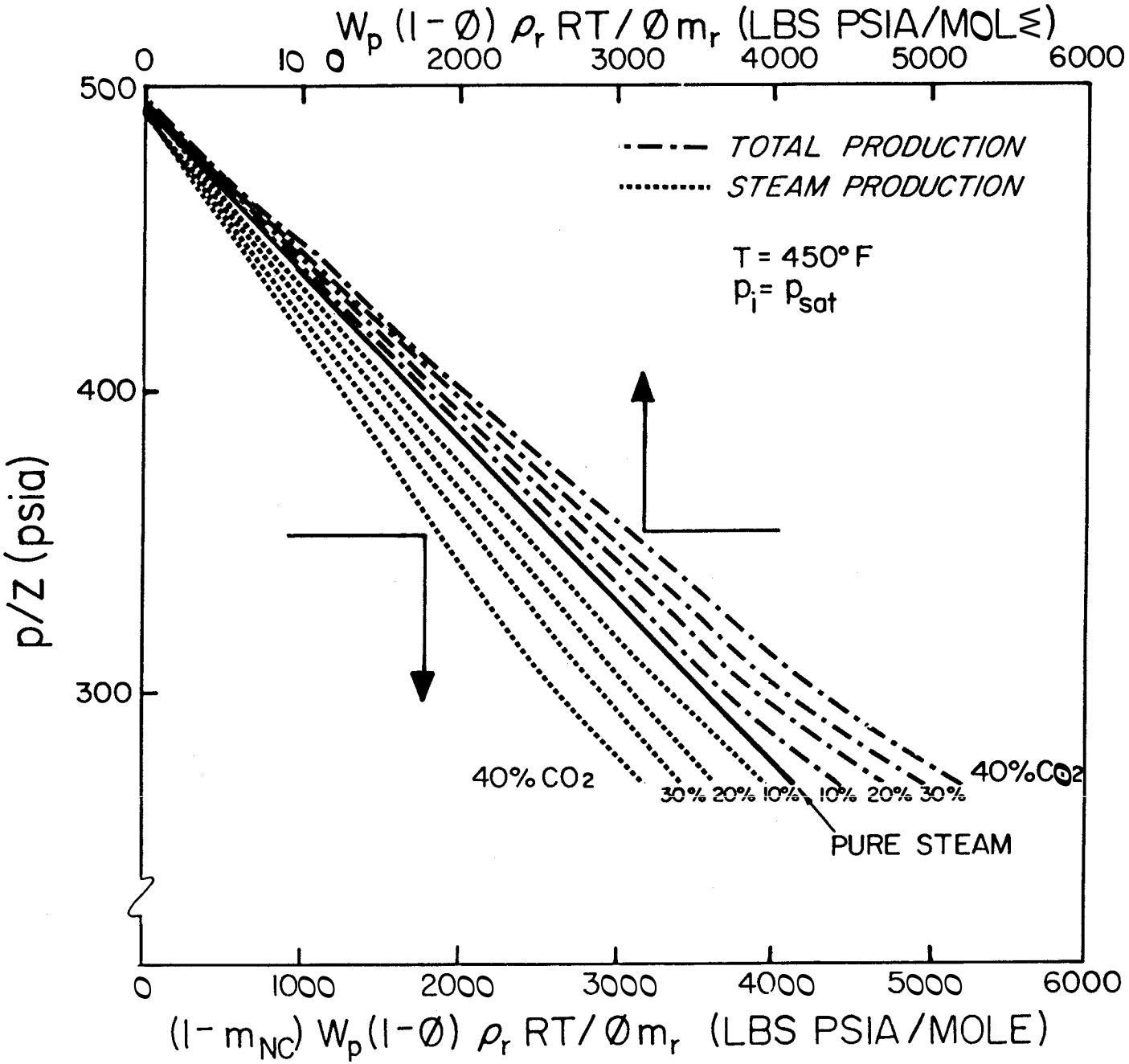

Figure 5-2 p/Z vs. Cumulative Production for Geothermal Reservoirs Containing CO_2.

noncondensable gas content is less than 30% (mass), the conventional approach of the straight line on the p/Z versus cumulative production curve should be adequate.

5.3 Steam and Adsorbed Water Reservoirs

When adsorbed water is considered, the pore volume contains both vapor and water molecules adsorbed on the grain surfaces as described earlier in this work. The material balance equation may be written taking into account the desorbing water. The amount of adsorbed water, X (lb moles/lb of rock), may be determined at any time during depletion of the reservoir with the equation derived from Hsieh's work:

$$X = \sigma(p/p^*) \qquad (3\text{-}1)$$

The material balance equation may then be written as:

$$MX_i\,(v_\ell - v_{\ell i}) + M(X_i - X)v_g + \frac{W_i(v_g - v_{gi})}{m_r} = \frac{W_p v_g}{m_r} \qquad (5\text{-}12)$$

The first term in this equation represents the decrease in the volume of the adsorbed fluid. The specific volume, v_ℓ, should probably be smaller than the liquid specific volume of water because the adsorbed water molecules form a dense phase on the rock surfaces. This term may be safely discarded because it is much smaller than the other three terms in Eq. 5-12.

The second and third terms represent the vaporization of the adsorbed fluid and the expansion of the initial vapor. Finally, the right hand side of the equation provides the cunulative production in terms of reservoir volumes.

Omitting the first term, and solving for W_p, Eq. 5-12 becomes:

$$\frac{W_p}{m_r} = M(X_i - X) + \frac{W_i}{m_r}\left(v_g - v_{gi}\right) \qquad (5\text{-}13)$$

Substituting Eq. 3-1 for $X_i - X$ and Eq. 5-5 for W_i, Eq. 5-13 becomes:

$$\frac{W_p}{m_r} = \frac{M\sigma(p_i - p)}{p^*} + \frac{\phi\,(v_g - v_{gi})}{(1-\phi)\rho_r v_g v_{gi}} \qquad (5\text{-}14)$$

Finally, substitution of Eq. 5-3 for v_g and v_{gi}, and rearranging Eq. 5-14 yields:

$$\frac{W_p}{m_r} = \frac{M\,\sigma p_i}{p^*} + \frac{M\,\phi\,(p_i/Z_i)}{(1-\phi)\rho_r RT} - \left[\frac{M\,\sigma Z}{p^*} + \frac{M\,\phi}{(1-\phi)\rho_r RT}\right] p/Z \qquad (5\text{-}15)$$

Equation 5-15 is analogous to Eq. 5-6. The second and the fourth terms on the right-hand side of Eq. 5-15 are identical to the right hand side of Eq. 5-6, while the first and the third terms are to account for the adsorption phenomenon.

Comparing the magnitude of the first term of the right-hand side versus the second, and the third versus the fourth discloses the importance of adsorption.

The value of σ for unconsolidated sandstones can be estimated from Fig. 3-2 as a function of temperature. Experiments by Hsieh (1980) for several consolidated sandstone cores, showed σ to be largely independent of temperature, and equal to 300×10^{-6} lb moles/lb of rock (g moles/g of rock).

The following variables may be considered for a typical vapor-dominated reservoir:

$T = 450^{o}F$, $p_i = 414$ psia, $p^* = 422.6$ psia

$\phi = 0.05$, $\rho_r = 165$ lb/ft^3, $Z_i = 0.868$

$\sigma = 300 \times 10^{-6}$ lb moles/lb of rock

Then:

$$\frac{M \sigma p_i}{p^*} = 5.29 \times 10^{-3} \text{ lb moles/lb of rock}$$

and:

$$\frac{M \phi (p_i/Z_i)}{(1-\phi)\rho_r RT} = 0.28 \times 10^{-3} \text{ lb moles/lb of rock}$$

Similarly:

$$\frac{M\sigma Z}{p^*} \approx 11 \times 10^{-6} \text{ lb/[(lb of rock)(psia)]}$$

while the fourth tern yields:

$$\frac{M\phi}{(1-\phi)\rho_r RT} = 0.59 \times 10^{-6} \text{ lb/[(lb of rock)(psia)]}$$

Thus, for a typical vapor-dominated reservoir, Eq. 5-15 may be simplified by dropping the second and fourth term, or the vapor depletion terms. The magnitude of the resulting error in W_p should be about 5% to 10%, depending on the value of the reservoir porosity.

Hence, as a reasonably close appraximation:

$$W_p \approx \frac{M\sigma}{p^*}(p_i - p)m_r \qquad (5\text{-}16)$$

Equation 5-16 is the equation of a straight line when the mass cumulative production is graphed against pressure, p.

For a vapor-dominated geothermal reservoir, it can be concluded that a graph of either p or p/Z against W_p may yield a straight line. The value of Z in the pressare and temperature ranges of geothermal interest varies little (from 0.8 to 0.9). Equation 5-16 provides the cumulative production per unit mass of rock. The total cumulative production can also be expressed by substituting $Ah(1-\phi)\rho_r$ for m_r. Eq. 5-16 becomes:

$$W_p = \frac{M \sigma Ah (1-\phi)\rho_r (p_i - p)}{p^*} \qquad (5\text{-}17)$$

In a graph of W_p as a function of p, the initial-fluid-in-place will be the value of W_p, corresponding to $p = 0$.

Significantly, Eq. 5-17 can be used to calculate bulk volume, **Ah,** if the porosity, ϕ , is **known** and if areal extent A is known or can be estimated, to calculate **thickness** h also.

5.4 A Revised Reservoir Engineering Study of The Geysers Geothermal Field

The preceding may be used to reevaluate data for the Big Geysers Area presented by Ramey (1968) in which he offered comprehensive reservoir engineering evaluation of the Rig Geysers area of The Geysers geothermal field. Table 5-1 reproduces the pressure production data, while Fig. 5-3 is a graph of both p/Z versus cumulative production and p versus cumulative production. An extrapolation of either of the straight lines drawn through the data result in an initial-mass-in-place of 2.4×10^{11} lbs. Both methods also agree in the estimation of cumulative production at the abandonment pressure of 60 psi (p/Z = 63): 158×10^9 lbs.

If The Geysers were presumed a gas reservoir, then the pore volume required could be calculated using the specific volume at 400°F and 194 psia, $v_g = 2.45$ ft^3/lb. This 'times 240×10^9 lbs gives 5.88×10^{11} ft^3 as the pore volume. Using Ramey's assumption of a drainage area of 4.792×10^6 ft^2 and a bulk reservoir porosity, the reservoir thickness could be calculated by:

TABLE 5-1

RIG GEYSERS **FIELD** SHALLOW ZONE CUMULATIVE PRODUCTION

AND RESERVOIR PRESSURE (From Ramey, 1970)*

Year	No. Wells	Steam Produced MM lb/yr.	M lb/hr.	Cumulative Stem MM lbs.	Avg. Res. Pressure psia**	Z	p/Z
1957	0	0	0	0	194	0.913	212
1957	5	1109.8	126.7	1,109.8	187	0.915	204
1958	5	3224.4	368.1	4,334.2	180	0.917	196
1959	10	3426.7	391.2	7,760.9	174	0.919	189
1960	10	4698.2	536.3	12,459.1	169	0.921	183
1961	10	4246.5	484.7	16,705.6	164	0.922	178
1962	10	4377.6	497.7	21,083.2	160	0.923	173
1963	13	5299.7	605.0	26,382.9	156	0.924	169
1964	12	6197.5	707.4	32,580.4	152	0.925	164
1965	3	5509.9	629.0	38,090.3	148	0.927	160
1966	7	4941.4	564.0	43,031.7	145	0.928	156
1967	7	3847.3	439.0	46,879.0	142	0.929	153

* Excludes production from original **wells** drilled in 1920's and production wells T-8, T-13 and T-14 after completion in deep zone.

** Measured at the wellhead.

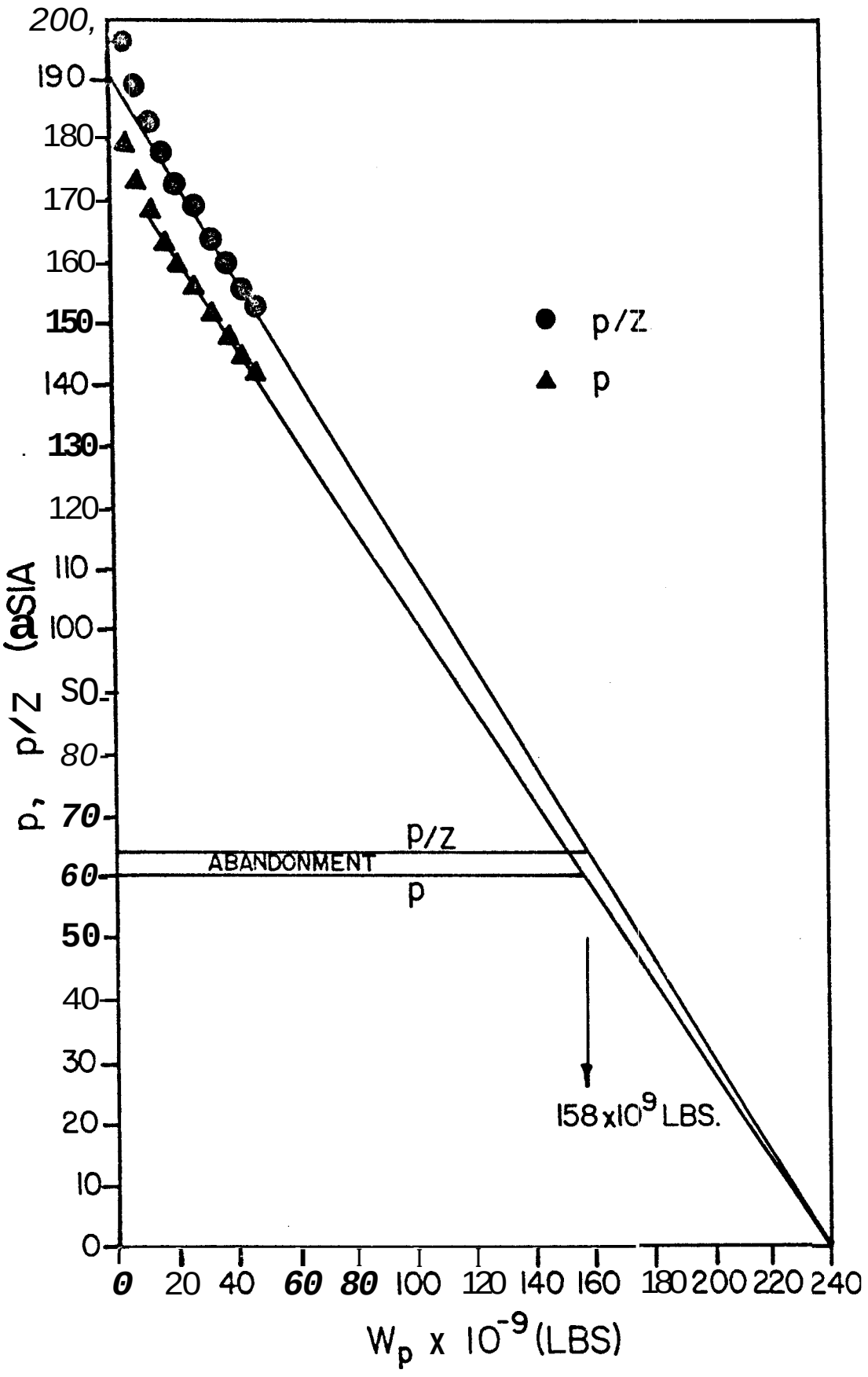

Figure 5-3 p and p/Z vs. Cumulative Production for the Big Geysers Zone at the Geysers. (p/Z after Ramey, 1968)

$$h = \frac{V_p}{A\phi} \qquad (5\text{-}18)$$

The results are given in Table 5-2.

TABLE 5-2

ESTIMATED RESERVOIR TEICKNESS FOR THE BIG GEYSERS AREA

ϕ	h(ft)
.01	1.23×10^7
.05	2.46×10^6
.10	1.23×10^6
.15	8.20×10^5
.20	6.15×10^5

These reservoir thicknesses are extremely large and they denote that the gas reservoir model would require a steam zone **plus** an underlying liquid-water zone or adsorbed water if a **more** reasonable thickness is to result.

Tne thickness of tne zone could be estimated. Assuming a constant temperature of 400°F, **one** can estimate the steam column required to exert sufficient pressure to reach the saturation

pressure. If p_i = 194 psia at the top and p_{sat} = 240 psia at 400°F at the bottom of the column, then Δp = 46 psis. The average specific volume is ((2.45 + 1.86)/2) or 2.155 ft^3/lb. Therefore:

$$h_g = 46 \times 144 \times 2.155 = 1.43 \times 10^4 \text{ ft.} \qquad (5\text{-}19)$$

If an increasing temperature gradient were assumed, then this depth would be even greater since the saturation pressure would be greater, hence a Δp would increase also.

The mass enclosed in this vapor zone can be calculated by:

$$\frac{Ah_g\phi}{v_g} = \frac{4.792 \times 10^6 \times 14300 \times \phi}{2.155} = 4.8 \times 10^8 \ \phi \text{ lbs} \qquad (5\text{-}20)$$

Even if the originally assumed drainage areas were underestimated by a factor of 10, and using a porosity of 1.5%, the mass contained in a steam-dominated zone would be about 2% of the total mass-in-place, 240 x 10^9 lbs (Fig. 5-3). The saturated liquid specific volume of, v_ℓ, at 400°F and 240 psia is 0.01864 ft^3/lb. Hence, the corresponding bulk volume of the liquid underlying this steam zone would be given by:

$$(V_b)_\ell = (W_i - \frac{Ah_g\phi}{v_g}) \frac{v_\ell}{\phi} = (240 - 4.8) \times 10^9 \times \frac{0.01864}{0.01500}$$

$$(V_b)_\ell = 2.92 \times 10^{11} \text{ ft}^3 \qquad (5\text{-}21)$$

Using A = 4.792 x 10^6 ft^2 the thickness of the underlying water zone is $(V_b)_\ell/A$ or 6.09 x 10^4 ft. Apparently, the originally assumed drainage area was underestimated significantly. Using a drainage area ten times the original, the water zone thickness reduces to about 6,000 ft.

The nodel extracted from Ramey's (1970) analysis requires a steam-dominated zone, over 14,000 feet thick, underlain by a bulk volume of 2.9 x 10^{11} ft^3 of liquid water. The thickness of this water zone depends on the estimated drainage area.

The required maximum bulk volume for the Big Geysers area, including adsorption, can be calculated using Eq. 5-17. Setting $W_p = W_i$ and $p = 0$ in that equation, and then solving for Ah, which is equivalent to V_b, we obtain:

$$V_b = Ah = \frac{W_i p^*}{M\sigma(1-\phi)\rho_r p_i} \qquad (5\text{-}22)$$

Substituting numerical values used earlier:

$$V_b = \frac{2.4 \times 10^{11} \times 240}{18 \times 300 \times 10^{-6} \times 0.985 \times 165 \times 194} = 3.4 \times 10^{11} \text{ ft}3 \qquad (5\text{-}23)$$

This is the maximum bulk volume required because the average value of the initial presure, p_i, must have been higher than 194 psia which is assumed as the pressure at the top of the reservoir. Using reservoir pressure of 240 psia, the bulk volume is only slightly higher than the required underlying liquid bulk volume calculated earlier in the last subsection (Eq. 5-21). The reservoir thickness calculated using adsorption would be only 17% greater than **the** thickness of the previously required underlying liquid reservoir.

5.5 Steam, Adsorbed Water and Noococdensable Gas Reservoirs

The reservoir pressure of a vapor-dominated reservoir containing CO_2 decreases during production from the initial value, p_i, to a current value, p. Referring to Eqs. 5-8 and 5-16, a volumetric balance can **be** stated:

$$\underbrace{\frac{M\sigma(p_i-p)v_g\, m_r}{p^*}}_{\text{Volume at } p \text{ of desorbed water}} + \underbrace{W_i\ [(1-m_{NCi})(v_g-v_{gi}) + m_{NCi}(v_{NC}-v_{NCi})]}_{\text{Expansion of original: steam and noncondensables } (CO_2) \text{ from } p_i \text{ to } p}$$

$$= \underbrace{W_p[\bar{m}_{NC}v_{NC} + (1-\bar{m}_{NC})v_g]}_{\text{volume at p of produced steam and noncondensables } (CO_2)} \qquad (5\text{-}24)$$

where W_i is the total initial mass of water vapor and noncondenseble gases present, and W_P is the totai cumulative mass production. Equation 5-24 is written in terms of average noncondensable gas concentrations, $\bar{m}_{NC}$ during the decline in reservoir pressure from p_i to p. **This** concentration will be reduced as water is continuously desorbing with declining pressure. The initial. vapor-in-place may be calculated using Eq. 5-10:

$$W_i = \frac{\phi}{(1-\phi)\rho_r \left[m_{NCi} v_{NCi} + (1-m_{NCi})\, v_{gi}\right]} \qquad (5\text{-}10)$$

Aft r algebraic manipulation, Eqs. 5-24 and 5-10 yield (see Appendix I for derivation):

$$\frac{W_p}{m_r} = \frac{\sigma Z p_i}{\left[\frac{\bar{m}_{NC} Z_{NC}}{M_{NC}} + \frac{(1-\bar{m}_{NC})Z}{M}\right] p^*}$$

$$+ \frac{\phi\, p_i/Z_i}{(1-\phi)\rho_r RT \left[\frac{1-\bar{m}_{NC}}{M} + \frac{\bar{m}_{NC}\, Z_{NC}}{M_{NC}\, Z}\right] \left[\frac{1-m_{NCi} + m_{NCi}\, \frac{Z_{NCi}}{Z_i}\, \frac{M}{M_{NC}}}{(1-m_{NCi}) + m_{NCi}\, \frac{Z_{NC}}{Z}\, \frac{M}{M_{NC}}}\right]}$$

$$- \frac{\sigma Z p}{\left[\frac{\bar{m}_{NC}\, Z_{NC}}{M_{NC}} + \frac{(1-\bar{m}_{NC})Z}{M}\right] p^*}$$

$$- \frac{\phi\, p/Z}{(1-\phi)\rho_r RT \left[\frac{1-\bar{m}_{NC}}{M} + \frac{\bar{m}_{NC}\, Z_{NC}}{M_{NC}\, Z}\right]} \qquad (5\text{-}25)$$

A simpler expression for W_P can be produced. The relative magnitudes of the four terms on the right-hand side of **Eq.** 5-25 can be estimated using typical geothermal reservoir values for the various parameters. The values used were:

$T = 910^{\circ}R$, $p_i = 414$ psia, $p^* = 422.6$ psia

$\phi = 0.05$, $\rho_r = 165$ lb/ft^3, $Z_i = 0.868$

$\sigma = 300 \times 10^{-6}$ lb moles/lb of rock, $m_{iCO_2} = 10$ mole%

The noncondensable gas is assumed to be CO_2 only. **Also** assumed are: $\bar{m}_{CO_2} = 5\%$; $Z_{CO_2} = 1$; and $Z = 0.872$. With these data, the terms can be evaluated:

First Term:

$$\frac{\sigma Z p_i}{\bar{m}_{NC} \frac{Z_{NC}}{M_{NC}} + (1-\bar{m}_{NC}) \frac{Z}{M} p^*} - \frac{(300\times10^{-6})(0.872)(414)}{[0.05 \frac{1}{44} + (1-0.05) \frac{0.872}{18}] 422.6}$$

$$= 5.43 \times 10^{-3} \text{ lb/lb of rock}$$

Second Term:

$$\frac{\phi\, p_i/Z_i}{(1-\phi)\rho_r RT\left[\frac{1-\bar{m}_{NC}}{M}+\frac{\bar{m}_{NC}\,Z_{NC}}{M_{NC}\,Z}\right]\left[\frac{1-m_{NCi}+m_{NCi}\,\frac{Z_i}{Z}\,\frac{M_{NC}}{M}}{(1-m_{NCi})+m_{NCi}\,\frac{Z_{NC}}{Z}\,\frac{M}{M_{NC}}}\right]} =$$

$$= \frac{(0.05)(414)\ /\ (0.868)}{(1-0.05)(165)(10.73)(910)\ (F_1)(F_2)} =$$

$$= 0.29\text{x}10^{-3}\ \text{lb/lb of rock}$$

where F_1:

$$= \left[\frac{1-0.05}{18}+\frac{(0.05)(1)}{(44)(0.872)}\right]$$

and F_2:

$$= \left[\frac{(1-0.1)+0.1\,\frac{(1)\ (18)}{(0.868)\ (44)}}{(1-0.1)+0.1\,\frac{(1)\ (18)}{(0.872)\ (44)}}\right]$$

Third Term:

$$\frac{\sigma Z p}{\frac{\bar{m}_{NC}\, Z_{NC}}{M_{NC}} + \frac{(1-\bar{m}_{NC})Z}{M}\; p^*}$$

$$= \frac{(300\times10^{-6})(0.872)\; p}{\left[\frac{(0.05)\;(1)}{44} + \frac{(1-0.05)(0.872)}{18}\right] 422.6}$$

$$= 1.31\times10^{-5}\ \textbf{(p)}\ \text{lb/lb of rock}$$

Fourth Term:

$$\frac{\phi\; p/Z}{(1-\phi)\rho_r RT\;\; \frac{1-\bar{m}_{NC}}{M} + \frac{\bar{m}_{NC}\, Z_{NC}}{M_{NC}\; Z}}$$

$$= \frac{(0.05)\; p\; /\; (0.872)}{(1-0.05)(165)(10.73)(910)\;\; \frac{1-0.05}{18} + \frac{(0.05)\;(1)}{(44)\;(0.872)}}$$

$$= 0.07\times10^{-5}\ \textbf{(p)}\ \text{lb/lb of rock}$$

As the second and fourth terms are much smaller than the first and third, Eq. 5-25 can be simplified to:

$$W_p \simeq \frac{\sigma Z (p_i - p) m_r}{\left[\bar{m}_{NC} \frac{Z_{NC}}{M_{NC}} + (1-\bar{m}_{NC}) \frac{Z}{M}\right] p^*} \qquad (5\text{-}26)$$

Equation 5-26 is not a linear function of p. For low noncondensable gas concentrations, it reduces to Eq. 5-16, while for large noncondensable gas concentrations, as in the Bagnore field in Italy which had an initial noncondensable gas concentration of over 80%, the shape of the curve is not linear.

The gas concentration, m_{NC}, is not constant because continuously desorbing water dilutes the gas phase. Thus, the produced gas concentration is a function of reservoir pressure. For an infinitesimal increment of total production, dW_p, this material balance applies:

$$m_{NC} dW_p = W dm_{NC} \qquad (5\text{-}27)$$

That is, the amount of noncondensable gas produced resulted in an equal reduction in the amount of noncondensable gases in the reservoir.

Moreover, the total production results in an equal amount of mass desorbing from the originally adsorbed water, or:

$$dW_p = dX \tag{5-28}$$

Differentiating Eq. **3-1** with respect to p:

$$dX = \frac{\sigma}{p^*} dp \tag{5-29}$$

Using Eq. 5-27 to substitute for dW_p and Eq. *5-29* to substitue for dX, Eq. 5-28 can be rearranged to become:

$$m_{NC} \frac{\sigma}{p^*} dp = W dm_{NC} \tag{5-30}$$

Separating variebles p and m_{NC}, this equation becomes:

$$\frac{\sigma}{p^* W} dp = \frac{dm_{NC}}{m_{NC}} \tag{5-31}$$

Integrating between p_i and p, and m_{NCi} and m_{NC}, and then solving for m_{NC}:

$$m_{NC} = m_{NCi} \, e^{-\sigma(p_i - p)/Wp^*} \tag{5-32}$$

Equation 5-32 is significant because it expresses the noncondensable gas concentration as a function of pressure. If the

only "non vapor" fluid present was in the forn of adsorbed water, then the preceding analysis is applicable. If underlying liquid water is present, then the concondensable gas concentration may not obey the analysis. In fact, the concentration may increase due to gas libsration from the liquid water zone. The theory presented here indicates that a graph of log m_{NC} versus p should yield a straight line. An application of this equation is provided in an example contained in subsection 5.6.

To develop a comprehensive material balance equation for a vapor-dominated geothermal reservoir whose noncondensable gas content decreases with increasing production, Eq. 5-26 is first written in differential form:

$$dW_p = \frac{\sigma \bar{Z}}{\left[\frac{m_{NC} Z_{NC}}{M_{NC}} + (1-m_{NC}) \frac{\bar{Z}}{\bar{M}} p^*\right]} dp \qquad (5\text{-}33)$$

Using Eq. 5-32 and introducing the constants:

$$K_1 = \frac{p^*}{M\sigma} \qquad (5\text{-}34)$$

$$K_2 = \frac{p^* \left[\frac{Z_{NC} m_{NCi}}{M_{NC}} - \frac{\bar{Z}\ m_{NCi}}{\bar{M}}\right] e^{-\sigma p_i / Wp^*}}{a\ 2} \qquad (5\text{-}35)$$

and

$$K_3 = \frac{\sigma}{W_p^*} \qquad (5\text{-}36)$$

Equation 5-33 becomes:

$$dW_p = \frac{dp}{K_1 + K_{2e}^{K_3 p}} \qquad (5\text{-}37)$$

Integration between 0 and W_p, and p_i and p yields:

$$W_p = \frac{1}{K_1 K_3} \log\left[\frac{K_1 + K_2 e^{K_3 p_i}}{K_1 + K_2 e^{K_3 p}}\right] - \left[\frac{p_i - p}{K_1}\right] \qquad (5\text{-}38)$$

Equation 5-38 with the associated Eqs. 5-34, 5-35 and 5-36 provides a comprehensive statement of the material bslance equation for a vapor-dominated geothermal reservoir containing a decreasing amount of noncondensable gases. When small quantities of gases are present, then the much simpler Eq. 5-17 should be used.

5.6 Application of the Carbon Dioxide Depletion Model to the Bagnore Field in Italy

The Bagnore field, near the Mt. Amiata Volcano in Central Italy began producing in 1959. The initial noncondensable gas content was more than 80% by weight, most of which was CO_2. During the first few years of Production, the noncondensable gss content dropped to about 10% by weight. Atkinson et al. (1978) presented a study of the

thercodynanic behavior of the Bagnore field. Their results indicated that a large accumulation of noncondensable gases was present in the reservoir, initially, and thst the CO_2 present could not be derived from local carbonate rocks.

Figure 5-4 is the pressure history of the reservoir from its initial state (1959) to the end of 1975, while Fig. 5-5 presents the noncondensabie gas content history of the sane reservoir. A development introduced earlier in this section, interprets the decline in the noncondensahle gas concentration as due to the desorbing liquid. Equation 5-29 suggests that a plot of log m_{NC} versus reservoir pressure should yield a straight line. For the Bagnore field, such a graph is presented in Fig. 5-6. The trends on the graph at early time do not obey the theory :presented earlier in this section. Instead, they show a slow decline at first followed by a rapid semi-log largely linear decline. The data nay indicate the presence of a noncondensable gas cap followed by gas production through the main reservoir where the dilution of the noncondensable gas concentrstion through fluid desorption becomes prevalent.

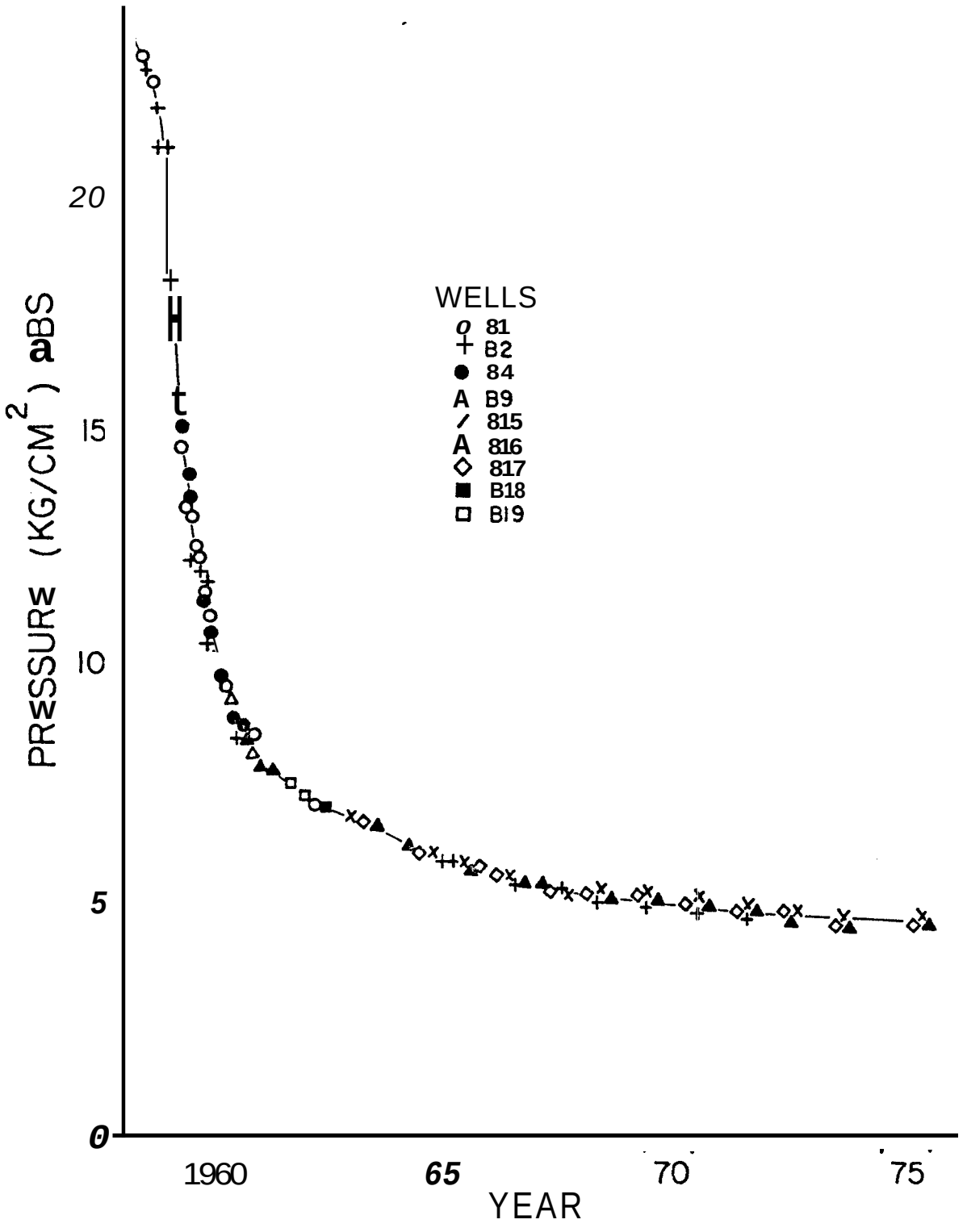

Figure 5-4 The Pressure History of the Bagnore Reservoir (From Atkinson et al.,1978)

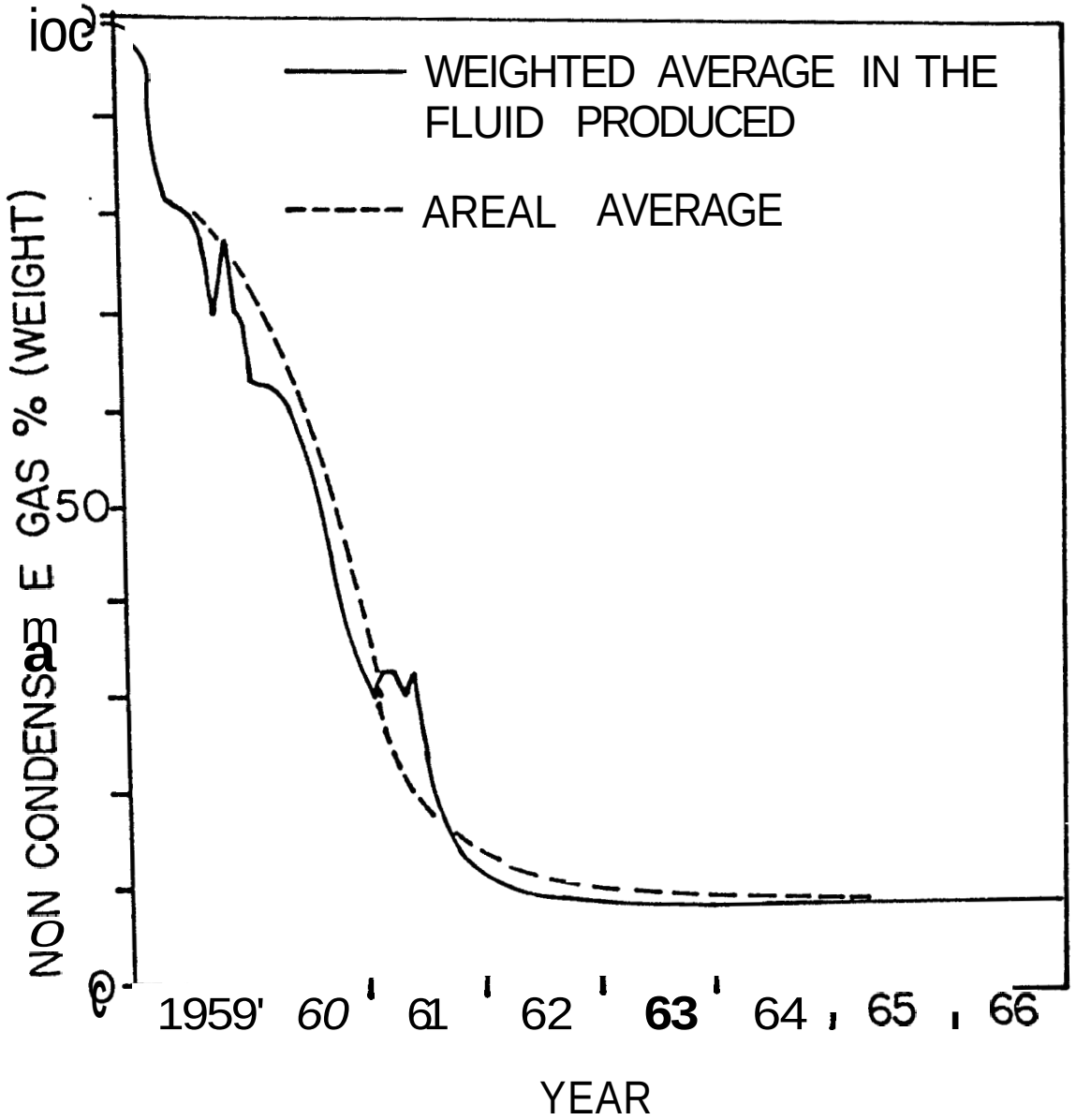

Figure 5-5 Noncondensable Gas History for the Bagnore Field

(After Atkinson et al. ,1978)

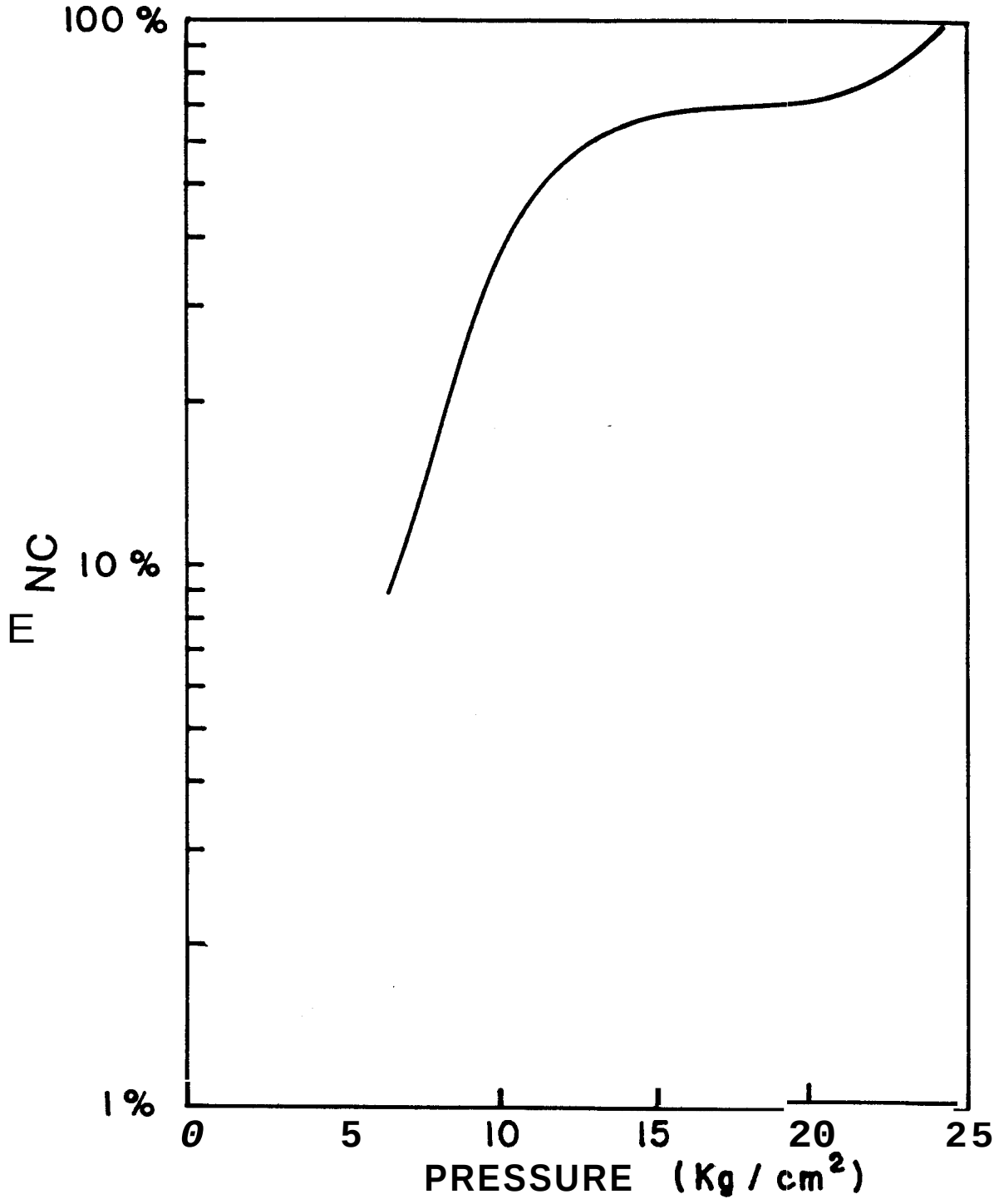

Figure 5-6 Semi-log Graph of the Nonocondensable Gas Concentration vs. Pressure for the Bagnore Field.

SECTION SIX

TRANSIENT PRESSURE WELL TEST ANALYSIS FOR A VAPOR-DOMINATED GEOTHERMAL RESERVOIR

In the previous section, new methods for interpreting field production data show that adsorption effects offer a plausible explanation for the enormous porosity-thickness products that result ftom conventional expansion material balance analysis for vapor-dominated geothermal reservoirs.

Indeed, if core samples can be used to determine the actual adsorption behavior and the matrix porosity for a particular geothermal formation, then the reservoir volume may be estisated from the methods previously detailed. In particular, for an estimated areal extent, a material balance can be used to estimate the average reservoir thickness, which for geothermal wells is generally not known because drilling through the entire steam zone is difficult and hazardous.

The production data required for material balance analysis may take cne or more years to develop. In the meantime, multiple well transient-pressure well tests may he used to estimate such formation parameters as the permeability-thickness and porosity-thickness products. These tests provide an inmediate method for determining an initial reservoir description.

In this section, the effects of adsorption will be incorporated into the model by Varren and Root (1963) for naturally-fractured fornstions. The resulting method of analysis provides a means for

disticguishing between fracture and matrix parameters which, when accompanied by experimental data or actual formation samples, provide a comprehensive formation description.

The derivation of the extension to the Warren and Root (1963) analysis requires certain assumptions that may be violated in the vapor-dominated system. To investigate the sensitivity of this model to departures from the necessary assumptions, a radial numerical model (without the assumptions) was developed. As will be shown in Section Seven, a numerical model validates the assumptions used in this section and, hence, justifies the simplified approach in the analytical model. Finally, in Section Seven, an example shows how the new method of analysis nay be applied to a geothermal well test using transient pressures generated by the numerical model.

Almost all geothermal reservoirs are found in naturally-fractured formations. In the analysis of a naturally-fractured model, most investigators consider two porous media regions both within the confines of a reservoir. Warren and 'Root (1963) used the term "primary porosity" when referring to that of the matrix and the term "secondary" when referring to that of the fractures. In the Warren and Root analysis, the fractured medium consists of a matrix where most of the fluid is stored, while the fractured zones serve as the main conduits for fluid flow.

In the case of geothermal steam, the adsorbed fluid contributes significantly to the total production. Since the matrix volume is

ordinarily much larger than the volume occupied. by fractures, the notion that most fluid is stored within the matrix is enhanced.

In the conventional two-porosity analysis of a fractured reservoir, the following assumptions are used:

(a) The system consists of a zone of primary porosity, ϕ_{ma} and a zone of secondary porosity, ϕ_f.

(b) Fractures are randomly oriented and evenly distributed throughout the reservoir.

(c) Pseudo-steady state occurs between elements of the matrix and the fractures, but no flow occurs through the matrix. In other words, fluid flows to the producing wells through a series of interconnecting fractures. While this assunption may be an idealization, it is not unlikely since the permeability of solid geothermal rocks has been experimentally measured at 1 md or less, while bulk well tests suggest permeabilities at 2 to 3 orders of magnitude higher. This implies a nuch higher transmissivity exclusively because of the fractures.

To account for adsorbed water in the vapor-dominated steam reservoir, the following two assumptions are added:

1. Fluid in the matrix can be found in two forms: steam or adsorbed water. The relative magnitude of these was discussed earlier. It was found that adsorbed water may include most of the fluid in a "vapor-dominated" geothermal reservoir.

2. Besorption of adsorbed water and the entire reservoir depletion is considered as an isothermal process.

Desorption of the liquid water takes place as the pressure in the matrix is lowered due to production of geothemal steam.

A balance of instantaneous mass rates can be written for macroscopically linear flow in the positive x direction in a fractured horizontal reservoir element of length dx and cross-sectional area A transverse to the direction of flow:

$$\bar{W}_{x+\delta x}A - \bar{W}_x A = \left[-\frac{\partial}{\partial t}(\rho\phi_f + \rho\phi_{ma})A\cdot\delta x\right] + \frac{\partial U}{\partial t} \qquad (6\text{-}1)$$

Outflow Rate - Inflow Rate = Sate of depletion of steam nass in element + Rate of H_2O desorption

in which $\bar{W}$ is the instantaneous mass rate of flow per unit of cross-sectional area, and is equal to the product of steam density and macroscopic velocity, (pv) .

Letting $\delta x \to 0$, the definition of a partial derivative leads to:

$$\bar{W}_{x+\delta x} - \bar{W}_x = \frac{\partial \bar{W}}{\partial x}\delta x = \frac{\partial(\rho v)}{\partial x}\delta x \qquad (6\text{-}2)$$

The first tern of Eq. 5-24 in the previous section is the volume of steam formed from desorbed water when the reservoir pressure drops from p_i to p in a mass m_r of reservoir rock. In the present instance, m_r is the mass of reservoir element under discussion, $(1-\phi_f-\phi_{ma})\rho_r\ A\cdot\delta x$ and p in Eq. 5-24 becomes p_{ma}. Hence, the value of the last term in Eq. 6-1 may be obtained by differentiating the desorption expression with respect to time:

$$\frac{\partial U}{\partial t} = \frac{\partial}{\partial t}\left[\frac{M\sigma}{p^*}(p_i-p_{ma})(1-\phi_f-\phi_{ma})\rho_r\ A\cdot\delta x\right] \qquad (6-3)$$

or further:

$$\frac{\partial U}{\partial t} = -\frac{M\sigma}{p^*}(1-\phi_f-\phi_{ma})\rho_r\frac{\partial p_{ma}}{\partial t}\ A\cdot\delta x \qquad (6-4)$$

Equation 6-2 may be used to substitute for the first two terms in Eq. 6-1, while Eq. 6-4 may be used to substitute for the term in Eq. 6-1 describing the water desorption. Finally, the differentiation in the bracketed expression on the right-hand side of Eq. 5-1 may be performed. All of the above result in:

$$\frac{\partial(\rho v)}{\partial x} = -\rho \frac{\partial \phi_f}{\partial t} - \phi_f \frac{\partial \rho}{\partial t} - \rho \frac{\partial \phi_{ma}}{\partial t} - \phi_{ma} \frac{\partial \rho}{\partial t}$$

$$- \frac{M\sigma}{p^*} (1-\phi_f-\phi_{ma}) \rho_r \frac{\partial p_{ma}}{\partial t} \qquad (6\text{-}5)$$

The left-hand side can be evaluated through application of the real-gas law and Darcy's law:

$$\frac{\partial(\rho v)}{\partial x} = \frac{\partial}{\partial x} \left[\left(\frac{M p_f}{ZRT} \right) \left(- \frac{k}{\mu} \frac{\partial p_f}{\partial x} \right) \right] \qquad (6\text{-}6)$$

$$= - \frac{Mk}{RT} \frac{\partial}{\partial x} \left(\frac{p_f}{\mu Z} \frac{\partial p_f}{\partial x} \right) \qquad (6\text{-}7)$$

Using srithmetic average values of p_f, μ, and Z as an approximation over the pressure range of interest, Eq. 6-7 can be simplified to:

$$\frac{\partial(\rho v)}{\partial x} = - \frac{Mk}{RT} \left(\frac{\bar{p}_f}{\bar{\mu} \bar{Z}} \right) \frac{\partial^2 p_f}{\partial x^2} = - \bar{\rho} \frac{k}{\bar{\mu}} \frac{\partial^2 p_f}{\partial x^2} \qquad (6\text{-}8)$$

The right-hand side of Eq. 6-5 can be simplified by assuming first that ϕ_f and ϕ_{ma} are independent of time, and secondly that either in the matrix pores or the fractures that:

$$\frac{\partial \rho}{\partial t} = \bar{c}\,\bar{\rho}\,\frac{\partial p}{\partial t} \qquad (6\text{-}9)$$

Thus, Eq. 6-5 can be written as:

$$\bar{\rho}\,\frac{k}{\bar{\mu}}\,\frac{\partial^2 p_f}{\partial x^2} = \phi_f\,\bar{c}\,\bar{\rho}\,\frac{\partial p_f}{\partial t} + \phi_{ma}\,\bar{c}\,\bar{\rho}\,\frac{\partial p_{ma}}{\partial t}$$

$$+ \frac{M\sigma}{p^*}\,(1-\phi_f-\phi_{ma})\rho_r\,\frac{\partial p_{ma}}{\partial t} \qquad (6\text{-}10)$$

Dividing through by $\frac{\bar{\rho}k}{\bar{\mu}}$ and rearranging, Eq. 6-10 can be put in the form:

$$\frac{\partial^2 p_f}{\partial x^2} = \frac{\bar{\mu}}{k}\,\phi_f\,\bar{c}\,\frac{\partial p_f}{\partial t} + \frac{\bar{\mu}\bar{c}}{k}\left[\phi_{ma} + \frac{\bar{p}M\sigma}{p^*\,\bar{\rho}}\,(1-\phi_f-\phi_{ma})\rho_r\right]\frac{\partial p_{ma}}{\partial t} \qquad (6\text{-}11)$$

For convenience and for comparison with the work of Warren and Root (1963), the bracketed quantity may be defined as the effective steam capacity, ϕ_{esc}, which can be used to substitute for the terms containing matrix porosity and adsorbed fluid.

$$\phi_{esc} = \phi_{ma} + \frac{M\sigma\,\bar{p}}{p^*\,\bar{\rho}}\,(1-\phi_f-\phi_{ma})\rho_r \qquad (6\text{-}12)$$

Equation 6-11 can be reduced to:

$$\frac{\partial^2 p_f}{\partial x^2} = \frac{\bar{\mu}\,\bar{c}}{k}\left(\phi_f \frac{\partial p_f}{\partial t} + \phi_{esc} \frac{\partial p_{ma}}{\partial t}\right) \qquad (6\text{-}13)$$

Equation 6-13 relies on an additional assumption that the steam compressibility is constant. Since steam is a real gas, the compressibility is a function of pressure, however, the vsriation in c_s is small over a wide range of pressures. A second assumption required by this model is that the steam density also does not vary much over the pressure range of interest. The numerical model to be described in Section Seven was used to validate these assumptions.

Equation 6-13 is analogous to the two-porosity analysis presented by Warren and Root (1963). Written in radial coordinates, Eq. 6-13 becomes:

$$\frac{\partial^2 p_f}{\partial r^2} + \frac{1}{r}\frac{\partial p_f}{\partial r} = \frac{\mu\bar{c}_s}{k}\left[\phi_f \frac{\partial p_f}{\partial t} + \phi_{esc} \frac{\partial p_{ma}}{\partial t}\right] \qquad (6\text{-}14)$$

This equation can be cast in dimensionless form by using a parameter, ω, , defined by:

$$\omega \triangleq \frac{\phi_f}{\phi_f + \phi_{esc}} \qquad (6\text{-}15)$$

The analogous expression in the Warren and Root (1963) analysis contained the fracture and matrix compressibilities, which can be omitted in the case of steam reservoirs because steam compressibility is larger by two orders of magnitude when corcpared with the fracture and matrix compressibilities. The compressibility of the adsorbed water is also small and it can be safely omitted.

The dimensionless form of Eq. 6-14 is then:

$$\frac{\partial^2 p_{Df}}{\partial r_D^2} + \frac{1}{r_D}\frac{\partial p_{Df}}{\partial r_D} \triangleq (1-\omega)\frac{\partial p_{Dma}}{\partial t_D} + \omega\frac{\partial p_{Df}}{\partial t_D} \qquad (6\text{-}16)$$

Equations of this type have been solved 'by a number of investigators besides Warren and Root, including Kazemi (1969), Streltsova (1976) and Mavor and Cinco (1979). The matrix-fracture interaction is described by Warren and Root (1963) and Mavor and Cinco (1979) as pseudo-steady state pressure relationship:

$$(1-\omega)\frac{\partial p_{Dma}}{\partial t_D} = \lambda(p_{Df} - p_{Dma}), \qquad (6\text{-}17)$$

where λ is the "dimensionless matrix/fracture permeability ratio" given by:

$$\lambda = \alpha \frac{k_{ma}}{k_f} r_w^2 \qquad (6\text{-}18)$$

and where α is a shape factor reflecting the geometry of the matrix elements.

Equation 6-17 is an approximation. Flow of fluid out of the matrix rock into the fractures must follow a pressure gradient within the matrix which cannot be represented by one pressure, p_{ma}. However, the error introduced by this approximation was assumed by Warren and Root (1963) to be insignificant.

Kazemi (1969) used a finite difference model which did incorporate a transient pressure distribution in the matrix. However, the differences between the two approaches were minor, thus, justifying Warren and Root's approximation of constant pressure within the matrix.

Equations 6-16 and 6-17 with initial and boundary conditions to account for the well and radial flow of unlimited extent are identical in form to the equations solved by Warren and Root

(1963). The solution of the pressure behavior for a constant flow rate well exhibits certain interesting features that have been used to calculate reservoir parameters. In particular, a graph of flowing pressure, p_{wf} versus log of time results in two distinct straight lines of the same slope, m, and separated by a vertical pressure difference, δp.

Warren and Root (1963) first related m, δp and ω, while Earlougher (1977) presented a practical example of their use in determining the permeability-thickness and the fracture pore volume. The relationship is:

$$\omega = 10^{(-\delta p/m)} \qquad (6\text{-}19)$$

In conventional two-porosity systems, a form similar to Eq. 6-15 is used to calculate the relationship between matrix and fracture porosity and associated reservoir volumes. However, in the case of fractured steam reservoirs, the following example shows that neglect of adsorption phenomena may result in the calculation of an unrealistic and significantly under-estimated value for the fracture porosity.

Example 6.1: Adsorption Effects in Two-Porosity Relationships

A comparison of results is presented to demonstrate the significance of the adsorption effect. In the first case, ϕ_f is

calculated ignoring adsorption phenomena. In the second case, ϕ_f is calculated for a slightly superheated geothermal **reservoir** with a temperature of 446°F (p^* = 405 psia), and a **pressure** of 397 psia. The density of steam is 0.98 lb/ft^3. The adsorption constant, a as estimated from Hsieh's work for unconsolidated sand is approximately 76 x 10^{-6} lb moles/lb of rock. For a typical sandstone, ρ_r = 155 lb/ft^3.

The values for ϕ_f including adsorption effects, were calculated using Eq. 6-15 and the definition of ϕ_{esc} given by Eq. 6-12. Substituting Eq. 6-15 into Eq. 6-12 and rearranging results in:

$$\phi_f = \frac{\omega[(1-\sigma')\phi_{ma} + \sigma']}{1 - (1-\sigma')\omega} \qquad (6-20)$$

where :

$$\sigma' = \frac{M}{\bar{c}_s} \frac{\rho_r}{\bar{\rho}_s} \frac{\sigma}{p^*} \qquad (6-21)$$

For $\bar{c}_s = \frac{1}{P} = 0.0362$, and a' = 0.228

$$\phi_f = \frac{\omega\,(0.772\phi_{ma} + 0.228)}{1 - 0.772\omega} \qquad (6-22)$$

Figure 6-1 is a graph of ϕ_f versus ϕ_{ma} with ω as the parameter. Dashed lines are the calculated values of ϕ_f ignoring adsorbed water. Solid lines represent calculated values of ϕ_f taking into account adsorbed water.

To demonstrate the significance of Fig. 6-1, assume that from a well test analysis, $\phi_{ma} \doteq 6\%$ and $\omega \doteq 0.3$. From the figure, a fracture porosity of 0.025 is obtained if adsorption is ignored, while the actual fracture porosity, taking into account adsorbed water is equal to 0.105, a four-fold increase.

Figure 6-1 shows that the error in the calculated value for the fracture porosity increases for smaller values of the matrix porosity, and for increasing values of a if adsorption effects are ignored.

Equation 6-20 can be used to calculate the fracture porosity from the standard two-porosity method of analysis provided that the matrix porosity and the value of the adsorption constant, σ, have been determined experimentally. In the next section, an example will illustrate the method for analyzing a geothermal well test for a vapor-dominated system which allows for the adsorption effects.

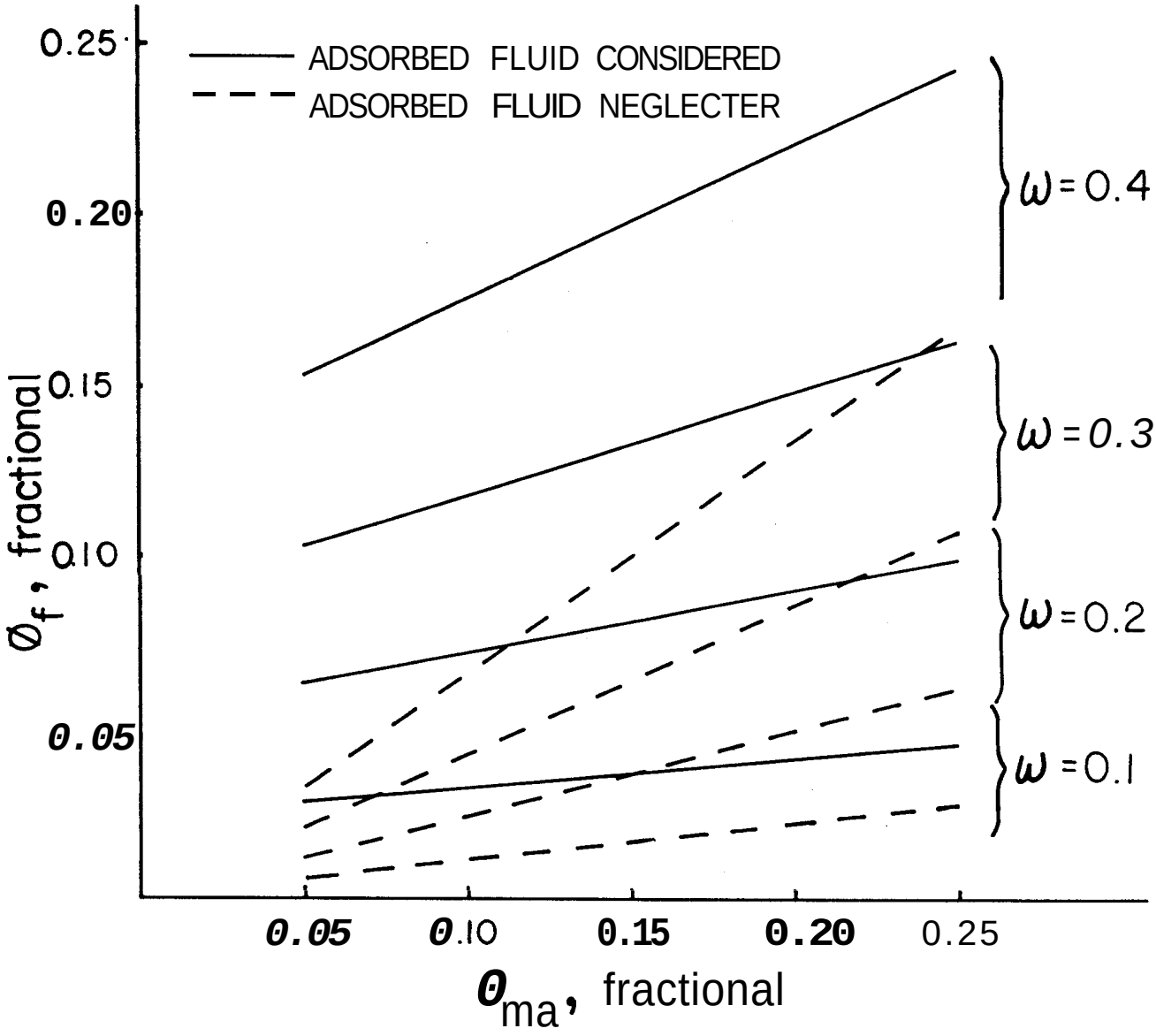

Figure 6–1 Crossplots of the Fracture and Matrix Porosities for Example 6–1 (Calculated Using Equation 6–22)

SECTION SEVEN

A NUMERICAL MODEL TO VERIFY THE ANALYTICAL SOLUTION DESCRIBING THE EEHAVIOR OF A GEOTHERMAL RESEEVOIR CONTAINING ADSORBED WATER

Derivation of the analytical solution for steam flowing in a two-porosity system, with or without adsorbed water, required assumptions that the steam density be approximately constant and the steam coapressibility be both small and constant. To check these assumptions, a radial finite difference model was developed. The derivation for the numerical model follows.

First, Eq. 6-7 is rewritten in radial coordinates:

$$\frac{\partial(\rho v)}{\partial x} = \frac{1}{r}\frac{\partial}{\partial r}\left[r\,\frac{p_f M}{RTZ}\,\frac{k_f}{\mu}\,\frac{\partial p_f}{\partial r}\right]$$

$$= \frac{k_f M}{\mu RT}\,\frac{1}{r}\,\frac{\partial}{\partial r}\left[r\,\frac{p_f}{Z}\,\frac{\partial p_f}{\partial r}\right] \qquad (7\text{-}1)$$

The vsriation in steam viscosity with pressure is neglected in Eq. 7-1. The transformation $u = \ln (r/r_w)$ results in the following:

$$\frac{\partial(\rho v)}{\partial x} = \frac{k_f M}{\mu RT}\,\frac{e^{-2u}}{r_w^2}\,\frac{\partial}{\partial u}\left(\frac{p_f}{Z}\,\frac{\partial p_f}{\partial u}\right) \qquad (7\text{-}2)$$

For the terms on the right hand side (RHS) of Eq. 6-5, the steam density is again approximated by the real gas law:

$$\frac{\partial}{\partial t}(\rho_s \phi) = \phi \frac{\partial p_s}{\partial t} = \phi \frac{\partial}{\partial t}\left(\frac{pM}{RTZ}\right) = \frac{\phi M}{RTZ}\frac{\partial p}{\partial t} \qquad (7\text{-}3)$$

Thus, results in the following expression for the right hand side of Eq. 6-5:

$$RHS = \frac{M}{RT}\left[\frac{\phi_f}{Z_f}\frac{\partial p_f}{\partial t} + \left[\frac{\phi_{ma}}{\bar{Z}_{ma}} + M_a \frac{RT}{M}(1-\phi_f-\phi_{ma})\,\rho_r \frac{\sigma}{p^*}\right]\frac{\partial p_{ma}}{\partial t}\right] \qquad (7\text{-}4)$$

Dividing both sides of the equation by the constant $k_f M/\mu RT r_w^2$ yields:

$$e^{-2u}\frac{\partial}{\partial x}\frac{p_f}{Z}\frac{\partial p_f}{\partial u} = \frac{158\mu r_w^2}{k_f}\left[\frac{\phi_f}{Z_f}\frac{\partial p_f}{\partial t} + \left[\frac{\phi_{ma}}{Z_{ma}} + RT\,(1-\phi_f-\phi_{ma})\,\rho_r \frac{\sigma}{p^*}\right]\frac{\partial p_{ma}}{\partial t}\right] \qquad (7\text{-}5)$$

The constant 158 is a conversion coefficient for the units used in Eq. 7-5 which are p (psi), μ (cp), r_w (ft), $T(^oR)$, ρ, ρ_r (lb/ft^3) σ (lb moles/lb of rock), t (hrs).

In Eqs. 7-4 and 7-5, $\bar{Z}$ refers to Z evaluated at the arithmatic average pressure over the time interval in the fracture for $\bar{Z}_f$, or in the matrix for $\bar{Z}_{ma}$.

The condition for flow between the matrix and fracture regions for an infinitessinal volume of matrix δV is given by:

$$\cancel{[(\rho_s v)_{in}}^{0} - (\rho_s v)_{out}] \, \delta s \Delta t = \Delta(\phi_{ma} \rho_s) \delta V$$

$$+ M_a \, (1-\phi_f-\phi_{ma}) \rho_r \frac{\sigma}{p^*} \Delta X \delta V \qquad (7\text{-}6)$$

where δs is the cross sectional area for flow out of the matrix. As there is no flow through the matrix, the term for flow into the matrix element is eliminated.

As in the Warren and Root (1963) analysis, the flow out of the matrix is approximated by a pseudo-steady state flow:

$$- (\rho_s v)_{out} \, \delta s = \rho_s \frac{k_{ma}}{\mu} (p_{ma}-p_f) \delta s' \qquad (7\text{-}7)$$

where $\delta s'$ is $\delta s/\ell$ and ℓ is the length the fluid must travel to leave the matrix element. The ratio of the volume of matrix to its surface area is given by the geometric factor, ω:

$$\omega = \delta s'/\delta V \tag{7-8}$$

By arguments analogous to the derivation of Eq. 7-5, the equation for flow between the matrix and fracture is given by:

$$\left[\frac{\phi_{ma}}{Z} + RT\ (1-\phi_f-\phi_{ma})\ \rho_r \frac{\sigma}{p^*}\right]\frac{\partial p_{ma}}{\partial t}$$

$$= \frac{-\alpha k_{ma}\ \bar{p}}{2(158)\mu\bar{Z}}\ (p_{ma}-p_f) \tag{7-9}$$

where $\bar{p} = (p_{ma} + p_f)/2$ and $\bar{Z}$ is evaluated at $\bar{p}$.

Equations 7-5 and 7-9 were solved numerically subject to the following initial and boundary conditions:

$$(p_{ma})_i = (p_f)_i = p_i \tag{7-10}$$

$$r_w \frac{p_f}{Z} \frac{\partial p_f}{\partial r}\bigg|_{r = r_w} \doteq \frac{12958 W \mu T}{M k_f h} \tag{7-11}$$

$$\lim_{r\to\infty} p_{ma} \doteq \lim_{r\to\infty} p_f \doteq p_i \tag{7-12}$$

Equation 7-5 was differenced using a variably implicit scheme similar to that used by Kazemi (1969):

$$\frac{e^{-2(j-1-\Delta u)}}{\Delta u^2}\Bigg[\alpha\left[a_j^{\,n} + \tfrac{1}{2}\left((p_f)_{j+1} - (p_f)_j\right) - a_j^{\,n} - \tfrac{1}{2}\left((p_f)_j - (p_f)_{j-1}\right)\right]^{n+1}$$

$$+ (1-\alpha)\left[a_j^{\,n} + \tfrac{1}{2}\left((p_f)_{j+1} - (p_f)_j\right) - a_j^{\,n} - \tfrac{1}{2}\left((p_f)_j - (p_f)_{j-1}\right)\right]^{n}\Bigg]$$

$$+ \frac{12958 W \mu T}{2 M k_f h(\Delta u)}\,\eta(j)$$

$$\doteq \frac{158\mu r_w^{\,2}\phi_f}{k_f}\left[\frac{\alpha}{Z_j^{\,n+1}} + \frac{(1-\alpha)}{Z_j^{\,n}}\right]\frac{\left((p_f)_j^{\,n+1} - (p_f)_j^{\,n}\right)}{(\Delta t)^{n+1}}$$

$$+ \frac{\omega k_{ma} r_w^{\,2}}{2k_f}\Bigg[\alpha b_j^{\,n+1}\left[(p_{ma})_j - (p_f)_j\right]^{n+1}$$

$$+ (1-\alpha)\, b_j^{\,n}\left[(p_{ma})_j - (p_f)_j\right]^{n}\Bigg] \tag{7-13}$$

where:

$$a_j^n = \frac{(p_f)_j}{Z_j}^n \quad \text{for } j = 2, \ldots, N$$

and

$$b_j^n = \left(\frac{\bar{p}_j}{Z_j}\right)^n$$

$$\bar{p}_j^n = [(p_{ma})_j + (p_f)_j]^{n/2}$$

$$\bar{Z}_j^n = Z(\bar{p}_j)^n$$

for $j = 1, \ldots, N$.

The time interval for each time step was increased by a constant multiplier. This results in approximately linear changes in the pressures throughout the grid, which in turn allows a simple estimation of the pressure distribution from one time step to the next.

The constant, 12958, multiplying the mass flow rate into the well is a conversion factor for the variables commonly used in steam flow [W (lbs/hr), μ(cp), T(^{o}R), k(md) and h(ft)] .

Finally,

$$\eta(j) = \begin{cases} 0, & j \neq 1 \\ 1, & j = 1 \end{cases}$$

Equation 7-13 provides a system of linear equations to solve for the p_j^{n+1} for j = 1, ..., N. However, the coefficients of each term in the equation are dependent on the solution for the p_j^{n+1}. Hence, the volumes for the p_j^{n+1} are estimated using a linear extrapolation of pressure with respect to the logarithm of At. The tridiagonal natrix for the system of equations is solved using the Thonas algorithm (Von Rosenburg, 1969) and the resulting new pressures are cocpared with the estimated values. If any calculated pressure differs from the estimate for any node, the calculated pressures are used to update the coefficients, and the system is solved again until the pressure converge to the solution.

After the tridiagonal natrix is solved, but before the coefficients are recalculated for another iteration, the matrix pressures, $(p_{ma})_j^{n+1}$, are calculated using a rearrangement of the following equation:

$$\frac{\phi_{ma}}{z_i^{n+1}} + RT\ (1-\phi_f-\phi_{ma})\ \rho_r \frac{\sigma}{p^*}\left[\frac{(\rho_{ma})_j^{n+1} - (\rho_{ma})_j^{n}}{(\Delta t)^{n+1}}\right]$$

$$= -\frac{\omega k_{ma}}{2(158\mu)}\left[\alpha\left[\frac{\bar{p}_j}{\bar{z}_j}\right]^{n+1}\ [(p_{ma})_j - (p_f)_j]^{n+1}\right.$$

$$\left. + (1-a)\left[\frac{\bar{p}_j}{\bar{z}_j}\right]^{n}\ [(p_{ma})_j - (p_f)_j]^{n}\right] \qquad \textbf{(7-14)}$$

As with the fracture pressures, estimates for the matrix pressures are replaced by calculated values. Convergence is achieved when both fracture and matrix pressures are unchanged within a preset tolerance from one iteration step to the next.

This scheme converges readily in three or four iterations except at very late tine because the near equality of the matrix and fracture pressures cause the calculation to be unstable.

A representative model run is shown in Fig. 7-1 showing results for 40 logarithmically spaced grid points, an initial time step of 1.10^{-12} days, and a time step increase factor of 1.58. (Initial time step choice is dependent on the parameters chosen for a particular model run. The time step increase factor is chosen arbitrarily for graphing convenience). Figure 7-1 shows that the transient pressures for the well form a trend that is qualitatively indistinguishable from the Warren and Root (1963) behavior. Curve 1 represents the

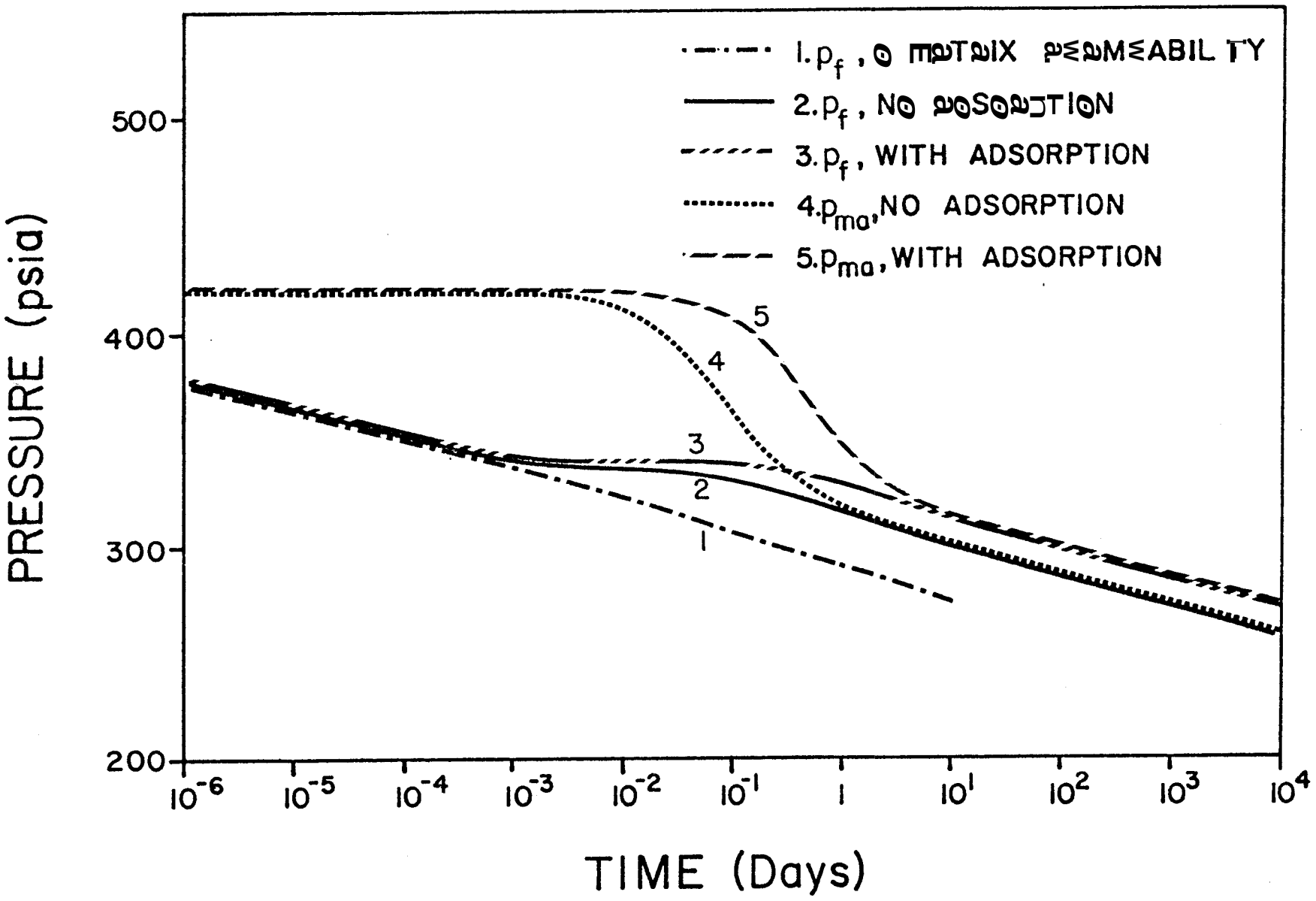

Figure 7-1 Pressure vs. Log Time in a Vapor-Dominated Fractured Reservoir when Adsorption are Considered

limiting case where there is no matrix permeability and the entire flow is through the fracture and with fluid stored in the fractures alone.

Curves 2 and 4 show the pressure response at the well for the fracture and matrix respectively when no adsorbed water is taken into account. As in the Warren and Root (1963) anslgsis, the fracture pressure shows a departure from the semi-log straight line with subsequent return to a parallel straight line. A similar trend is demonstrated here in carves 3 and 5. These results, that include the adsorption phenomenon, also exhibit an early time departure from the straight line with a subsequent return. This departure is significantly prolonged when corcpared to a model where the adsorption phenomenon is neglected.

The values of the reservoir parameters used for the model run in Fig. 7-1 are listed in Table 7-1. Tabulated results of the simulated data appear in Table 7-2.

Example 7.1: Example Calculation of Reservoir Parameters from Simulated Field Data

To explain the implications of these results better, the data shown in Fig. 7-1 are analyzed using the extension of the Warren and Root (1963) analysis described earlier in this section. Figure 7-2 is a semi-log graph of simulated flowing bottom hole pressures of a vapor-doninated geothermal well.

TABLE 7-1

Reservoir Parameters to Generate Figure (7-1)

Fracture Permeability, k_f = 1000 md

Matrix Permeability, k_{ma} = 1 md

Fracture Porosity, ϕ_f = 0.001

Matrix Porosity, ϕ_{ma} = 0.05

Density of Rock ρ_r = 165.4 lb/ft^3

Reservoir Temperature, T = 910^{o}R

Formation Thickness, h = 200 ft

Wellbore Radius r_w = 0.316 ft r_w

Initial Pressure, p_i = 420 psia

Warren and Root Geometric Factor, a = 0.01

Adsorption Coefficient, σ = 78x10^{-6} moles/lb of rock

Steam Flow Rate, W = 150,000 lb/hr

Saturation Pressure, p^* = 423 psia

Steam Viscosity, μ = 0.02 cp

TAELE 7-2

Simulated Pressure Response in a Two-Porosity

Vapor-Dominated Reservoir

	Without Adsorption (Warren & Root, 1963)		With **Adsorption**	
t (days)	p_f	p_{ma}	p_f	p_{ma}
10^{-6}	378	420	378	420
10^{-5}	365	420	365	420
10^{-4}	351	420	351	420
10^{-3}	341	419	342	420
10^{-2}	338	411	340	419
10^{-1}	336	351	339	408
10^{0}	316	318	328	365
10^{1}	302	302	315	315
10^{2}	285	285	300	300
10^{3}	275	275	289	289
10^{4}	260	250	270	270

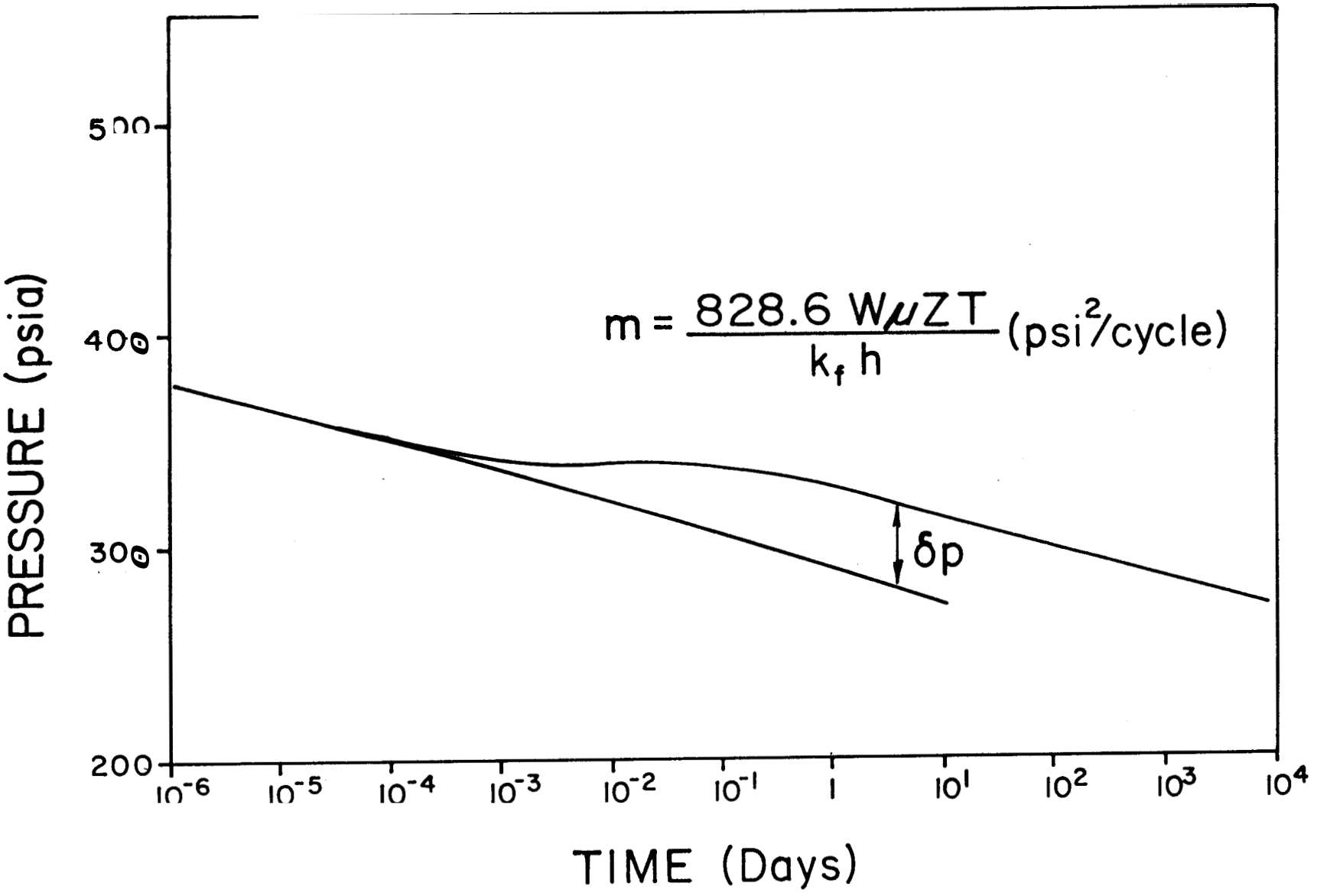

Figure 7-2 Semi-log Graph of the Pressure Data for Example 7-1.

The slope of the straight line (between t = 1 and t = 10) is approximately 17 psi/cycle or 9605 psi^2/cycle:

$$m = \frac{14914.8 W \mu \bar{Z} T}{M k_f h} \qquad (7\text{-}15)$$

$$\bar{p} = \frac{291 + 274}{2} = 282.5, \quad \bar{Z} = 0.893 \qquad (7\text{-}16)$$

hence:

$$k_f = \frac{14914.8 \times 150{,}000 \times 0.02 \times 0.893 \times 910}{9605 \times 18 \times 200} = 1{,}051 \text{ md} \qquad (7\text{-}17)$$

The pressure difference between the two straight lines is δp = 42 psi. Hence:

$$\omega = 10^{-\delta p/m} = 10^{-42/17} = 0.0034 \qquad (7\text{-}18)$$

Recalling that:

$$\omega \doteq \frac{\phi_f}{\phi_f + \phi_{esc}} \qquad (6\text{-}15)$$

and that:

$$\phi_{esc} \doteq \phi_{ma} + M\,(1-\phi_f-\phi_{ma})\,\frac{\rho_r}{\bar{\rho}_s}\,\frac{\sigma\bar{p}}{p^*} \qquad (6\text{-}12)$$

and then using these data:

$\phi_{ma} \doteq 0.05$, $\sigma \doteq 78$ (from **Hsieh)**
$\rho_r \doteq 165.4$ lb/ft^3, $p^* = 423$ psia
$\bar{p} \doteq 282.5$ **psia** and $\bar{\rho}_s \doteq 0.58$ lb/ft^3 (from steam tables)

ϕ_{esc} can be calculated.

$$\phi_{esc} \doteq 0.05 + 0.267\,(1-\phi_f-0.05) \qquad (7\text{-}19)$$

Using **Eq.** 6- 15 and Eq. 7-19, the fracture porosity can be calculated as $\phi_f \doteq 0.00103$. The actual value **used** to calculate the data was 0.001.

If the adsorption phenomenon were ignored, and if $\phi_{esc} - \phi_{ma} \doteq 0.05$, then the value of ϕ_f calculated via Eq. 6-15 would be much smaller, i.e., $\phi_f \doteq 0.00017$.

The computer csde for the numerics1 model i3 presented in Appendix II.

CONCLUSIONS

Considerable evidence points to the presence of adsorbed water in vapor-dominated geothermal roservoirs. In this work, conventional models for material balance and pressure transient behavior were extended to incorporate the effects of adsorption. The new models developed in this report make possible reasonable icterpretations of conventional reservoir engineering tests as applied to vapor-dominated geothermal systems.

The form of the material balance equation provided here suggests that the most appropriate method for estimating reserves, when adsorption effects dominate, is a graph of pressure (instead of p/z) versus cumulative production. Because the z factor for steam varies only slightly in the range of interest for vapor-dominated geothermal reservoirs, the graph of p/z versus cusulative production results in an equivalent estimate. The same procedure, including adsorption effects, could also apply to natural gas.

For steam, although the ultimate estimate for mass in place is the same whether or not the material balance incorporates adsorption, the allowance for adsorbed water in the vapor zone profoundly affects the estimation of reservoir bulk volume and results in a more realistic calculation of the reservoir thickness than previous models.

Another implication of the new material balance equation is that the nonccndecsable gas content in the produced fluid provides additional evidence of the adsorption phenomenon. The model

indicates that the concentrstion of noncondensable gases is an exponential function of pressure. A graph of the logarithm of the gas concentration veraus pressure for the Bagnore field resulted in a straight line.

Incorporetion of the adsorption phenomenon into a model for well test analysis required certcin assumptions about the nature of flow in the geothermal formation. Since the known vapor-dominated reservoirs are highly fractured, the model by Warren and Root (1963) was used as the basis for this analysis. A new method for applying the Warren and Root (1963) theory was developed which allows a more accurate estimation of the fracture porosity.

REFERENCES

Atkinson, P., Celati, R., Corsi, R., Kucuk, F. and Ramey, H. J., Jr.: "Thermodynamic Behaviour of the Bagnore Geothermal Field," Geothermics V. 7, pp. 185-208, 1978.

Barelli, A., Brigham, W. E., Cinco, H., Economides, M. J., Miller, F. G., Ramey, H. J., Jr. and Schultz, A.: "Pressure Drawdown Analysis for the Travale 22 Well", Proc., Fourth Workshop on Geothermal Reservoir Engineering, Stanford University (1978) 165.

Barelli, A., Celati, R., Manetti, G. and Neri, G.: "Buildup and Back-Pressure Tests on Italian Geothermal Wells", Proc., Second U.N. Symposium on the Development and Use of Geothermal Reservoirs, San Francisco, LBL, University of California (1975).

Bilhartz, H. L., Jr.: "Fluid Production from Geothermal Steam Reservoirs", M.S. Report, Stanford University (1971).

Brigham, W.E. and Morrow, W.E.: "p/Z Behavior for Geothermal Steam Reservoirs", Paper SPE 4899, presented at the 41th California Regional Meeting of the S.P.E., April 4-5, 1974.

Brunauer, S., Emmett, P. H. and Teller, E.: "Adsorptisn of Gases in Multimolecular Layers", J. Amer. Chem. Soc. (1938) 63, 309-319.

Cady, G. V.: "Model Studies of Geothermal Fluid Production", Ph.D. Thesis, Stanford University, 1969.

Chicoine, S.D.: "A Physical Model of a Geothermal System - Its Design and Construction and Its Application to Reservoir Engineering," Engineer's Thesis, Stanford University, 1975.

Cinco-Ley, H., Economides, M. J. and Miller, F. G.: "A Parallelepiped Model to Analyze the Pressure Behavior of Geothermal Steam Wells Penetrating Vertical Fractures", Paper SPE 8231, presented at the 54th Annual Fall Technical Conference & Exhibition, SPE of AIME, Las Vegas, Sept. 23-26, 1979.

Denlinger, R. P.: "Geophysical Constraints on The Geysers Geothermal Field, Northern California", Ph.D. Thesis, Stanford University, 1979.

Derjauguin, B. V.: "Effect of Lyophile Surfaces on the Properties of Boundary Liquid Films", Discussion of the Farady Society (1966) 42, 109-119.

Earlougher, R. C., Jr.: "Advances in Well Test Analysis", Society of Petroleum Engineers, 1977, p. 131.

Economides, M. J., Ogbe, D., Miller, F. G., Cinco-Ley, H. and Fehlberg, E. L. : "Pressure Buildup Analysis of Geothermal Steam Wells Using Parallelepiped Model", J. of Fet. Tech. V. 34, no. 4, April 1982, pp. 925-929.

Ellis, A. J.: "Partial Molal Volume of Boric Acid in Water at High Temperature", Chem. Commun. (1966) 21.

Ellis, A. J. and Golding, R. M.: "The Solubility of Carbon Dioxide Above 100°C in Water and in Sodium Chloride Solutions", Amer. Jour. Science 621, (1936), pp. 47-60.

Fisher, L. R. and Israiachvili, J. N.: "Direct Experimental Verification of the Kelvin Equation for Capillary Condensation", Nature (1979) 277, pp. 548-549.

Grant, M. A.: "Water Content of the Kawah-Kamojang Geothermal Reservoir", Geothermics, V. 8, 1979.

Greenwood, H. J.: "The Compressibility of Gaseous Mixtures of Carbon Dioxide and Water Between 0 and 500 Bars Pressure and 450 and 800°C", Amer. J. Sci., (1969) 267A.

Gringarten, A. C. and Ramey, H. J., Jr.: "The Use of Source and Green's Functions in Solving Unsteady-Plow Problems in Reservoirs", SPE J. (October 1973), p. 285.

Gringarten, A. C., Ramey, H. J., Jr. and Raghavan, R.: "Unsteady-State Pressure Distributions Created by a Well with a Single Infinite-Zonductivity Vertical Fracture", SPE J. (Aug. 1974), p. 347.

Henniker, J. C.: "The Depth of the Surface Zone of a Liquid", Rev. of Modern Physics (1949) 21, pp. 322-341.

Herkelrath, W. N. and Moench, A. F.: "Laboratory Investigations of the Physics of Steam Flow in a Porous Medium", U.S.G.S. Open File Report 82-95, 1982.

Herkelrath, W.N., Koench, A.F. and O'Neal, C.F., 11,:" Laboratory Investigstion of Steam Plow in a Porous Medium", (In press), Water Resources Research, 1983.

Horne, R. S., Day, A. F., Young, R. P. and Yu, N. T.: "Interfacial Water Structure: The Electrical Conductivity Under Hydrostatic Pressure of Particulate Solids Permeated with Aqueous Electroiyte Solution", Eletrochimica Acta (1968) 13, pp. 397-406.

Houghton, G., McLean, A. M. and Ritchie, P. D.: "Compressibility, Fugacity and Water-Soiubility of Carbon Dioxide in Region 0-36 atm and 0-100°C", Chem. Engr. Sci. (1971) 61, 1971.

Hsieh, C. : "Vapor Pressure Lowering in Porous Media", Ph.D. Thesis, Stanford University, 1980.

Hsieh, C.H. and Ramey, H.J., Jr.,: "Vapor-Pressure Lowering in Geothermal Systems", SPE J., (February 1983) p. 157.

Katz, D.L. , Cornell, D., Kobayashi, R., Poettmann, F.H. , Vary, J.A. , Elenbass, J.R. and Weinaug, C.F.: Handbook of Natural Gas Engineering, McGraw Hill Co., N.Y., 1959.

Kazemi, H.: "Pressure Transient Analysis of Naturally Fractured Reservoir with Uniform Fracture Distributions", Trans. AIME (1969), 246, pp. 451-462.

Kennedy, G. C.: "Pressure-Volume-Temperature Relstions in CO_2 at Elevated Tenperatures and Pressures", Amer. J. of Sci. (1954), 252, p. 2.

Langmuir, I.: "The Constitution and Fundamental Properties of Solids and Liquids, Part I. Solids", J. Amer. Chem. Soc. (1916) 38, pp. 2221-1195.

Macias-Chapa, L.: Radon Emanation in Geothermal Reservoirs, Engineer's Thesis, Stanford University, 1981.

Malinin, S. D.: "The System Water-Carbon Dioxide at High Temperatures and Pressures", Geochemistry (1959) 3, pp. 292-306.

Malinin, S. D. : "Theraodynsmics of the H_2O-CO_2 System", Geochemistry International (1974), pp. 1060-1085.

Mavor, M. J. and Cinco-Ley, H.: "Transient Pressure Behavior of Naturally Fractured Reservoirs", Paper SPE 7977, Presented at the 1979 California Regional Meeting, Society of Petroleum Engineers.

Muskat, M.: "The Flow of Homogeneous Fluids Through Porous Media", J. W. Edwards, Inc., Ann Arbor, Mich. (1946).

Pritchett, J. W., Garg, S. K., Brownell, D. H., Jr. and Levine, H. B. : "Geohydrological Environmental Effects of Geothermal Power Production - Phase I", Systems, Science and Software Report No. SSS-R-75-2733, La Jolla, California, Sept. 1975.

Ramey, H. J., Jr.: "A Reservoir Engineering Study of The Geysers Geotnermal Field", Submitted as Evidence, Reich and Reich, Petitioners v. Commissioner of Internal Revenue, 1969 Tax Court of the United States, 52, T.C. No. 74 (1970).

Ramey, H. J., Jr. and Gringarten, A. C.: "Effects of High-Volume Vertical Fracture on Geothermal Steam Well Behavior", Proc., Second

U.N. Symposium on the Development and Use of Geothermal Reservoirs, San Francisco, 1975.

Sanyal, S.K. (1980) Personal Communication.

Streltsova, T. D.: "Hydrodynamics of Groundwater Flow in a Fractured Formation", Water Resources Research, V. 12, no. 13 (June, 1976), p. 405.

Strobel, C. J.: "Kodel Studies of Geothermal Fluids Production from Consolidated Porous Kedia", Engineering Thesis, Stanford University, 1373.

Sutton, F. M.: "Pressure-Tenperature Curves for a Two-phase Mixture of Water and Carbon Dioxide", New Zealand J. of Sci. (1976) 19, pp. 297-301.

Tekenouchi, G. and Kennedy, G. C.: "The Binary System H_2O-CO_2 at High Temperatures and Pressures", Amer. J. of Sci. (1964) 272, pp. 1055-1074.

Todhede, K. and Franck, E. U.: "Das Zweiphasengebiet und die Kristshe Kurve im System Kohlendioxid-Wasser bis zu Drucken. vo 7500 bar", Zeitschrift fur Physikalische Chemie (neue Folge) (1963) 37, pp. 387-401.

Von Rosenburg, D. V.: "Methods for the Numerical Solution of Partial Differential Equations", p. 113, Elsevier, New York, 1969.

Warren, J. E. and Root, P. J.: "The Behavior of Naturally Fractured Reservoirs", SPE. J. (Sept. 1963), pp. 245-255.

Whiting, R.L. and Ramey, H.J., Jr.: "Application of Material and Energy Balances to Geothermal Steam Production", J. Pet. Tech., (July 1969), pp. 893-900.

Zyvoloski, G.A. and O'Sullivan, M.J.: "Simulation of a Gas-Dominated Two-Phase Geothermal Reservoir", SPE. J. (Feb. 1980), pp. 52-95.

NOMENCLATURE

A	= area, ft^2
B	= formation volume factor
C_r	= rock heat capacity, BTU/lb°F
	= total compressibility, psi^{-1}
c	= constant in BET equation
f	= fugacity of the gas above the liquid
G	= initial gas-in-place, SCF
G_p	= cumulative production gas, SCF
h	= reservoir thickness, ft
h_g	= enthalpy of vapor, BTU/lb
h_i	= initial enthalpy of fluid, BTU/lb
h_ℓ	= enthalpy of liquid, BTU/lb
$h_{\ell g}$	= heat of vaporization, BTU/lb
h_p	= enthalpy of produced fluid, BTU/lb
k	= permeability, md
K	= vapor-liquid equilibrium constant
K_H	= Henry's law constant
m	= slope of pressure vs log t curve
m_a	= mass of adsorbed fluid, lb
m_g	= mass of vapor, lb
m_{NC}	= mass fraction of noncondensable gases
m_r	= mass of rock
M	= molecular weight
n	= moles

p = pressure, psi (bars)

p^* ≐ vapor pressure, psi (bars)

p_c = critical pressure, psi (bars)

p_r ≐ reduced pressure

q ≐ flow rate, bpd

Q_s ≐ net heat conducted into reservoir, BTU

r ≐ radial distance, ft

R ≐ gas constant, 10.73 ft^3 psi/mole ^oR

t ≐ time, hrs

T ≐ absolute temperature, ^oR (^oK)

T_c ≐ critical temperature, ^oR (^oK)

T_i ≐ initisl temperature, ^oF

T_r ≐ reduced temperature

u_x = velocity

v ≐ specific volume ft^3/lbm

V_b ≐ bulk volume, ft^3

v_l ≐ specific volume liquid, ft^3/lb

V_p ≐ pore volume, ft3

V ≐ volume, ft3

W ≐ steam flow rate, lb/hr

W_e ≐ fluid influx, lbs

W_i ≐ initial steam-in-place, lbs.

W_L ≐ lost fluid, lbs

W_p ≐ steam cumulative production, lbs

x ≐ liquid mole frsction

X = adsorbed water, lb moles/lb of rock (g mole/g of rock)

y = vapor mole fraction

z = total mole fraction in a gas mixture

Z = gas deviation factor

Symbols

a = geometric factor in Warren and Root analysis

β = relative pressure in BET equation

γ = activity coefficient

δp = pressure departure between two straight lines in a two-porosity system

δs = cross sectional area of flow

Δt = shut-in time

λ = dimensionless matrix/fracture permeability ratio

μ = viscosity, cp

ρ = density, lb/ft^3 (g/cc)

σ = adsorption/desorption curve slope

ϕ = porosity

ω = ratio of fracture porosity to total porosity

Subscripts

a = adsorbed

D = diaensionless

e = influx

esc = effective steam capacity

f = fracture

g = gas

i = initial

l = liquid

ma = matrix

NC = noncondensable

P = produced

r = rock

s = steam

sc = standard condition

w = well

wf = flowing bottom hole

ws = shut-in bottom hole

APPENDIX I

Development of Eq. 5-25

Equation 5-25 may be developed by substituting the right-hand side of Eq. 5-10 for W_i in Eq. 5-24, then dividing by the coefficient of W_p in Eq. 5-24 and solving the resulting equation for W_p. This results in:

$$W_p \doteq \frac{M\sigma\,(p_i-p)v_g\,m_r}{p^*\,(\bar{m}_{NC}v_{NC} + (1-\bar{m}_{NC})v_g)} \qquad \text{(A)}$$

$$\left.\begin{aligned} &+ \frac{\phi m_r}{(1-\phi)\rho_r\,(m_{NCi}\,v_{NCi} + (1-m_{NCi})v_{gi})} \\ &\cdot \frac{[(1-m_{NCi})(v_g-v_{gi}) + m_{NCi}\,(v_{NC}-v_{NCi})]}{(\bar{m}_{NC}\,v_{NC} + (1-\bar{m}_{NC})\,v_g)} \end{aligned}\right\} \qquad \text{(B)}$$

(I-1)

The term labelled A in Eq. I-1 may be further expanded:

$$A \doteq \frac{M\sigma p_i v_g}{p^*\,(\bar{m}_{NC}\,v_{NC} + (1-\bar{m}_{NC})v_g|} - \frac{M\sigma p v_g}{p^*\,(\bar{m}_{NC}\,v_{NC} + (1-\bar{m}_{NC})v_g)}$$

(I-2)

Substitution of the values of the specific volumes with the equivalent expressions from the real gas law result in:

$$A = \frac{\sigma p_i Z \left(\frac{RT}{p}\right)}{p^* \left[\bar{m}_{NC} \frac{Z_{NC}}{M_{NC}} \left(\frac{RT}{p}\right) + (1-\bar{m}_{NC}) \frac{Z}{M} \left(\frac{RT}{p}\right)\right]} - \frac{\sigma p Z \left(\frac{RT}{p}\right)}{p^* \left[\bar{m}_{NC} \frac{Z_{NC}}{M_{NC}} \left(\frac{RT}{p}\right) + 1-\bar{m}_{NC} \frac{Z}{M} \left(\frac{RT}{p}\right)\right]} \qquad \text{(I-3)}$$

The first term in Eq. I-3 is the same as the first term in Eq. 5-25, while the second term in Eq. I-3 is the same as the third term in Eq. 5-25.

Similarly, the term labelled B in Eq. I-1 may be expanded into:

$$B = \frac{\phi}{(1-\phi)\rho_r \left(\bar{m}_{NC} v_{NC} + (1-\bar{m}_{NC}) v_g\right)} \left[\frac{m_{NCi} v_{NC} + (1-m_{NCi}) v_g}{m_{NCi} v_{NCi} + (1-m_{NCi}) v_{gi}} - 1\right] \qquad \text{(I-4)}$$

Again, substitution of the values of the specific volumes by the equivalent expression from the real gas lsw results in:

$$B = \frac{\phi}{(1-\phi)\rho_r \left[\bar{m}_{NC} \frac{Z_{NC}}{M_{NC}} \frac{RT}{p} + (1-\bar{m}_{NC}) \frac{Z}{M} \frac{RT}{p} \right]}$$

$$\left\{ \frac{m_{NCi} \frac{Z_{NC}}{M_{NC}} \left(\frac{RT}{p}\right) + (1-m_{NCi}) \frac{Z}{M} \left(\frac{RT}{p}\right)}{m_{NCi} \frac{Z_{NCi}}{M_{NC}} \left(\frac{RT}{p_i}\right) + (1-m_{NCi}) \frac{Z_i}{M} \left(\frac{RT}{p_i}\right)} - 1 \right\} \qquad \text{(I-5)}$$

or:

$$B = \frac{\phi}{(1-\phi)\rho_r \frac{RTZ}{pM} \left[\bar{m}_{NC} \frac{Z_{NC} M}{M_{NC} Z} + (1-\bar{m}_{NC}) \right]}$$

$$\left\{ \frac{\frac{RTZ}{pM} \left[m_{NCi} \frac{Z_{NC}}{M_{NC}} \frac{M}{Z} + (1-m_{NCi}) \right]}{\frac{RTZ_i}{p_i M} \left[m_{NCi} \frac{Z_{NCi}}{M_{NC}} \frac{M}{Z_i} + (1-m_{NCi}) \right]} - 1 \right\} \qquad \text{(I-6)}$$

Simplifying:

$$B \doteq \frac{\phi\, p_i/Z_i}{(1-\phi)\rho_r RT\left[\bar{m}_{NC}\frac{Z_{NC}}{M_{NC}Z} + \frac{(1-\bar{m}_{NC})}{M}\right]} \cdot \left\{ \frac{1}{\left\{\frac{(1-m_{NCi}) + m_{NCi}\frac{Z_{NCi}}{Z_i}\frac{M}{M_{NC}}}{(1-m_{NCi}) + m_{NCi}\frac{Z_{NC}}{Z}\frac{M}{M_{NC}}}\right\}} - 1 \right\} \qquad (I\text{-}7)$$

Equation 1-7 supplies the second term in Eq. 5-25, while the subtracted unity in the last term results in the fourth term of Eq. 5-25.

APPENDIX II

Computer Code

```
c RADIAL STEAM MODEL WITH ADSORBED WATER
      IMPLICIT REAL*8(A-H,O-Z)
      COMMON /COEF/A(100),B(100),C(100),D(100),DP(100)
&     ,DMAT(100)
      REAL*8 KMA,KF,MW
      COMMON /PRESS/PF(100),PFP(100),PM(100),PMP(100)
      COMMON /VAR/SIGMA,KMA,KF,VIS,W,MW,H,RW,ALPHA,PSTAR,
&    DROCK,PHIMA,PHIF,PI
      COMMON /EXTRA/ R(100),THETA,NU,DELT,RDT,TIME,JCOUNT
      COMMON /TEMP/ T
      DIMENSION RD(100),BETA(100),GAM(100)
      INTEGER COUNT
      JCOUNT=0
C NUMBER OF RADIAL GRID SPACES
      NU=40
      NUP=NU+1
      NUM=NU-1
      NUR=8
C INPUT DATA
      SIGMA=-.01
      KMA=1.
      KF=1000.
      VIS=.02
      W=-150000.
      T=910.
      MW=18.
      H=200.
      RW=.316
      ALPHA=0.
      PSTAR=423.
      DROCK=165.4
     PHIMA=.05
      PHIF=.001
      RED=1.D7
      PI=420.
C INITIAL DELTA TIME
      DELT=1.D-12
      PTIME=.1D-6
C INITIAL TIME(DAYS)
      TDI=10.*DELT
C TIME INCREASE FACTOR
      RDT=10.**0.2
C NUMBER OF TIME STEPS TO BE COMPUTED
      NTS=200
C NUMBER OF ITERATIONS ALLOWED
      ITCOUNT=30
      ERROR=.001
      ERRORM=.01
C PRINT OUT TIME STEPS WHICH ARE MULTIPLES OF MCOUNT
      MCOUNT=5
C RELAXATION PARAMETER
      THETA=0.5
C INITIALIZE ARRAYS
C
```

```
C
      DO 10 I=1,NUP
      PF(I)=PI
      PFP(I)=PI
      PM(I)=PI
   10 PMP(I)=PI
      DELT=DELT/RDT
C COMPUTE CONSTANT RADIAL COEFFICIENTS
      DELU=DLOG(RED)/NU
      DELUX=DELU*DELU
      TEMP=DEXP(DELU)
      TEMPX=TEMP*TEMP
      RD(1)=RW
      R(1)=1./DELUX
      DO 20 I=1,NUM
      RD(I+1)=RD(I)*TEMP
   20 R(I+1)=R(I)/TEMPX
      PRINT 101
  101 FORMAT (' NODE SPA ING')
      PRINT 102,(RD(I),I=1,NU,NUR)
  102 FORMAT (' ',10E12.4)
      TIME=TDI
      DO 500 COUNT=1,NTS
C EXTRAPOLATE VALUES FOE PF,PM AT TIME STEP J+1
C
C
      TD=TIME
      TIME=RDT*TIME
      DELT=TIME-TD
C LINEAR EXTRAPOLATION
   29 PO 30 I=1,NUP
      PFP(I)=2.*PF(I)-PFP(I)
      PMP(I)=2.*PM(I)-PMP(I)
      IF (DABS((PMP(I)-PFP(I))/PMP(I)) .LT. ERROR) PMP(I)=PFP(I)
   30 COMTIMUE
      IF (COUNT .EQ. 1) CALL ABCDCON
      JCOUNT=1
C
C
C TURN THE CRANK
C
      DO 35 I=1,NU
   35 D(I)=DP(I)
      D(1)=D(1)-0.5*12958.*W*VIS*T/DELU/MW/H/K F
      DO 400 IT=1,ITCOUNT
      ICON=0
      GO TO 51
   36 B(NU)=0.
C CALCULATE COEFFICIENTS FOR THOMAS ALGORITHI!
C
      BETA(1)=B(1)
      GAM(1)=(D(1)+DMAT(1))/E (1)
      DO E0 I=2,NU
      BETA(I)=B(I)-A(I)*C(I-1)/BETA (I-1)
```

```
      GAM(I)=(D(I)+DMAT(I)-A(I)*GAM(I-1))/BETA(I)
   40 CONTINUE
C
C BACK SUBSTITUTION
      PFP(NU)=PI
      DO 50 K=1,NUM
      I=NU-K
      TEMP=PFP(I)
      PFP(I)=GAM(I)-C(I)*PFP(I+1)/BETA(I)
      IF (DABS(PI-PFP(I)) .LT. 1.D-9) PFP(I)=PI
      TEMPI=DABS(TEMP-PFP(I))/TEMP
      IF (PFP(I) .GT. PI) PFP(I)=PI
      IF (TEMPI .GT. ERROR) ICON=1
   50 CONTINUE
      GO TO 56
   51 COEF=158.*VIS*RW*RW/KF
      DO 55 I=1,NU
      PMAVG=(PM(I)+PMP(I))*0.5
      PPAVGM=(PMP(I)+PFP(I))*0.5
      PAVGM=(PM(I)+PF(I))*0.5
      C1=10.73D-6*T*(1.-PHIMA-PHIF)*DROCK*ALPHA/PSTAR
      C1P=C1
      C1=(C1+PHIMA/Z(PMAVG))/DELT
      C2=SIGMA*KMA*PAVGM/(2.*158.*VIS*Z(PAVGM))
      C2P=SIGMA*KMA*PPAVGM/(2.*158.*VIS*Z(PPAVGM))
      TEMP=PMP(I)
      PMP(I)=(C1*PM(I)-THETA*C2P*PFP(I)+(1.-THETA)*C2
&     *(PM(I)-PF(I)))/(C1-THETA*C2P)
      IF (DABS(PI-PMP(I)) .LT. 1.D-9) PMP(I)=PI
      IF (PMP(I) .GT. PI) PMP(I)=PI
      TEMPI=DABS(TEMP-PMP(I))/TEMP
      IF (TEMPI .GT. ERROR1) ICON=1
      C1P=(C1P+PHIMA/Z((PMP(I)+PM(I))*0.5))/DELT
      DMAT(I)=COEF*C1P*(PMP(I)-PM(I))
   55 CONTINUE
      CALL ABCDCON
      GO TO 36
C TEST FOR CONVERGENCE
   56 CONTINUE
      IF (ICON .EQ. 0) GO TO 60
  400 CONTINUE
   60 PRINT 120,IT,COUNT
  120 FORMAT (' ',I2,' ITERATIONS ON TIME STEP ', I3)
      CALL ABCDCON
C
C ITERATION COMPLETE
C
      IF(MOD(COUNT,MCOUNT) .NE. 0) GO TO 490
      IF (TIME .LT. PTIME) GO TO 490
      PRINT 119,TIME
  119 FORMAT (' TIME = ',E12.4,' DAYS')
      PRINT 123
  123 FORMAT (' FRACTURE PRESSURE DISTRIBUTION')
      PRINT 124,(PFP(I),I=1,NU,NUR)
```

```
  124 FORMAT (' ',10E12.4)
      PRINT 125
  125 FORMAT (' MATRIX PRESSURE DISTRIEUTIOI!')
      PRINT 124, (PMP(I),I=1,NU ,MUR)
C
C
C
  490 DO 80 I=1,NUP
      TEMP=PFP(I)
      PFP(I)=PF(I)
      PF(I)=TEMP
      TEMP=PMP(I)
      PMP(I)=PM(I)
   80 PM(I)=TEMP
  500 CONTINUE
      STOP
      END
C
C
C
      DOUBLE PRECISION FUNCTION Z(P)
      IMPLICIT REAL*8(A-H,O-Z)
      COMMON /TEMP/ T
      R=10.73
      Z=18.*P/((.01267+.00212*P)*R*T)
      RETURN
      END
C
C
C
      SUBROUTINE ABCDCOH
      IMPLICIT REAL*8(A-H,O-Z)
      COMMON /COEF/A(100),B(100),C(100),D(100),DP(100)
     REAL*8 KMA,KF,MW
      COMMON /PRESS/ PF(100),PFP(100),PM(100),PMP(100)
      COMMON /VAR/SIGMA,KMA,KF,VIS,W,MW,H,RW,ALPHA,PSTAR
&     ,DROCK,PHIMA,PHIF,PI
      COMMON /TEMP/ T
      COMMON /EXTRA/ R(100),THETA,NU,DELT,RDT,TIME,JCOUNT
      COEF=158.*VIS*RW*RW/KF
      DO 10 I=1,NU
      PAVGM=(PFP(I)+PFP(I-1))*0.5
      PAVG=(PFP(I+1)+PFP(I))*0.5
      APM=PAVGM/Z(PAVGM)
      IF(I .EQ. 1) APM=0.
      AP=PAVG/Z(PAVG)
      DD=PHIF*((THETA/Z(PFP(I))+(1.-THETA)/Z(PF(I))))/DELT
      A(I)=THETA*APM*R(I)
      C(I)=THETA*AP*R(I)
      B(I)=-R(I)*THETA*(AP+APM)-COEF*DD
      IF (JCOUNT .EQ. 1) DD=DD*DELT/((RDT-1.)*TIME)
      DP(I)=-R(I)*(1.-THETA)*(AP*(PFP(I+1)-PFP(I))-APM*(PFP(I)-
&     PFP(I-1)))-COEF*DD*PFP(I)
   10 CONTINUE
```

```
      DP(NU)=R(NU)*(APM*PI-(1.-THETA)*APM*PFP(NU-1))
      RETURN
      END
```